AEROSOLIZED INFLUENZA INFECTION DURING LATE GESTATION PREGNANCY IN THE FERRET MODEL

by

Emily Rachel Gage

B.S., University of Vermont, 2009

Submitted to the Graduate Faculty of

the Department of Infectious Diseases and Microbiology

Graduate School of Public Health in partial fulfillment

of the requirements for the degree of

Master of Science

University of Pittsburgh

2013

UNIVERSITY OF PITTSBURGH

GRADUATE SCHOOL OF PUBLIC HEALTH

This thesis was presented

by

Emily Rachel Gage

It was defended on

April 3, 2013

and approved by

Todd A. Reinhart, Sc.D.
Professor
Department of Infectious Diseases and Microbiology
Graduate School of Public Health
University of Pittsburgh

Amy L. Hartman, Ph.D.
Assistant Research Professor
Department of Infectious Diseases and Microbiology
Graduate School of Public Health
University of Pittsburgh

Jay K. Kolls, M.D.
Professor
Department of Pediatrics and Immunology
School of Medicine
University of Pittsburgh

Thesis Director: Kelly Stefano Cole, Ph.D.
Associate Professor
Department of Immunology
School of Medicine
University of Pittsburgh

Kelly Stefano Cole, Ph.D.

**AEROSOLIZED INFLUENZA INFECTION DURING LATE GESTATION
PREGNANCY IN THE FERRET MODEL**

Emily Gage, M.S.

University of Pittsburgh, 2013

ABSTRACT

Human pregnancy is known to predispose women to disproportionate morbidity and mortality from influenza infection. Limited investigation has been performed to understand the mechanism(s) of increased risk. Investigation of a pregnant ferret model was undertaken using aerosolized 2009 pH1N1 influenza. Pregnant ferrets demonstrated worse clinical disease and increased pro-inflammatory cytokine gene expression levels, notably IL-6 and IL-10 in the lung and at the maternal/fetal interface but not the spleen. Influenza virus was detected by semi-quantitative RT-PCR in many tissues including the placenta and kits but not the uterus of the non-pregnant ferrets, suggesting placental-fetal transmission. No obvious difference in lung pathology was observed between the pregnant and age-matched controls. Further model development is warranted to elucidate mechanisms that cause greater disease during pregnancy and effects of maternal disease on fetal outcomes. Ultimately, this model would further aid in investigating countermeasures against influenza during pregnancy. The public health significance of this study is that by establishing a pertinent influenza pregnant animal model, answers to translational questions about the effectiveness of therapeutics and when treatment would be most effective could be investigated, potentially lowering the amount of lives lost, hospitalization rates, and economic burden caused by this health disparity.

TABLE OF CONTENTS

LIST OF TABLES

LIST OF FIGURES

ACKNOWLEDGMENTS

First and foremost, I would like to thank my advisor, Dr. Kelly Stefano Cole, and the rest of my thesis committee, Drs. Amy Hartman, Todd Reinhart and Jay Kolls for their support and guidance with this project. I would also like to thank honorary committee members, Drs. Richard Beigi and Doug Reed for their contributions to my project. I would like to extend a large thank you to my classmates and friends, in particular my labmate Amy Caroline, for all their support and camaraderie throughout my time here. Lastly, I would like to thank my family for their love and steadfast support.

1.0   INTRODUCTION

1.1   VIRAL ORIGINS OF PANDEMIC H1N1

Influenza A virus is a zoonotic pathogen that continuously circulates through animal hosts, such as humans, birds, horses, dogs and pigs[1,2]. This virus has a segmented, negative-sense, single stranded RNA genome that typically encodes 11-12 proteins[1,3]. Generally it is thought that simultaneous infection of a single cell by two distinct influenza A viruses can cause reassortment of genes and result in the generation of a novel influenza strain, which can lead to human pandemics[1,3].

Typically, influenza A viruses are subtyped based on their hemagglutinin (HA) and neuraminidase (NA) glycoproteins[4]. Currently, there are virus strains from 16 HA subtypes and nine NA subtypes circulating in birds, and two virus subtypes circulating in humans[1]. Evolution of human seasonal influenza typically undergoes antigenic drift characterized by point mutations in the HA and NA glycoproteins, necessitating a new yearly influenza vaccine and causing yearly epidemics. Larger changes in the HA subtype, typically caused by reassortment of two strains results in antigenic shift and the emergence of novel strains that can cause devastating pandemics[2].

In April 2009, a novel H1N1 influenza A virus infected humans, possibly originating from a domestic pig population in Mexico[5–7]. By the end of April, the World Health

Organization (WHO) had issued a Global Outbreak Alert as a result of laboratory-confirmed human cases of swine influenza A/H1N1 in the USA and Mexico. Two months later, the U.S. Centers for Disease Control and Prevention (CDC) and WHO declared this outbreak of swine H1N1 influenza a pandemic. The genome of pandemic H1N1 2009 (pH1N1) had never been previously seen in humans but there is evidence its' predecessor circulated in pigs for years prior to its initial zoonotic transmission[6].

1.2   EPIDEMIOLOGY OF PANDEMIC H1N1

Pandemic H1N1 emerged in early April 2009 in Vera Cruz, Mexico, quickly spreading to California and later, worldwide[8]. The emergence of 2009 pH1N1 came as a surprise because no surveillance is currently conducted in Mexico's domestic pig population[9]. By April 2010, over 214 countries reported laboratory-confirmed A (H1N1) 2009 cases[10]. Most countries in the southern hemisphere immediately reported an increase in pandemic influenza compared to seasonal strains, but this happened more gradually in northern hemisphere countries[11]. Between April 2009 and August 2010, it has been estimated that 1-3 billon people worldwide were infected (15-45% of the world's population)[12]. Mathematical models estimate that over 201,000 respiratory deaths and 83,000 cardiovascular deaths were associated with pH1N1 globally[12].

In the United States, an estimated 61 million cases of pH1N1 resulted in approximately 274,000 hospitalizations and 12,470 deaths, primarily occurring in individuals with underlying medical conditions[12,13]. However, unlike most influenza seasons where the burden and severity occurs among older individuals, a unique characteristic of pH1N1 was the shifting of the burden of disease to children and young adults[10]. Children under the age of 5 had the highest rate of

severe disease leading to hospitalization[9]. It has been suggested that older age groups may have been exposed to a genetically similar virus previously, and had developed partial immunity[14], Subsequent seroprevalence studies demonstrated that 33% of humans over the age of 60 years old had cross-reactive antibodies to pH1N1[15].

Pregnant women, especially those in their second and third trimesters, were also disproportionately affected. Estimates suggest that one third of all pregnant women in the US with confirmed pH1N1 were hospitalized, with their most common symptom being acute respiratory distress often requiring mechanical ventilation[16]. Of pregnant women hospitalized in the US, 23.3% were admitted to the intensive care unit (ICU) and 8% died[16,17]. At any given time, pregnant women make up approximately 1% of the US population, but during the pandemic, they accounted for 6.3% of general hospitalizations, 5.9% of ICU admissions, and 5.7% of deaths, underscoring that pregnant women were disproportionately affected[17]. Preterm delivery was also commonly reported, exceeding 30% when compared to a baseline level of 9.6%[17]. Many of the neonates did require hospitalization, but this was largely due to preterm birth, and not due to transmission of influenza. Among 45 infants tested by various methods of influenza detection in different locations, only 6 positive tests were reported, suggesting a small likelihood of fetal transmission[17].

1.2.1 Influenza Vaccine and Treatment

The influenza vaccine is considered to be one of the most important tools for preventing the spread, and mitigating the impact, of influenza morbidity and mortality[18,19]. Children aged 6 months to 4 years had the highest vaccine coverage rate at 33%[20]. The CDC strongly recommended vaccination for individuals afflicted with high-risk conditions, health care

personnel, pregnant women, and adults caring for children under the age of 6 months.[19]. Even with these highly publicized recommendations, only an estimated 46% of pregnant women, 12% of those with high-risk conditions, and 22% of health care personnel received the H1N1 vaccine by early January 2010 in the US[20].

The predominate immunogen in the inactivated vaccine is the hemmaglutinin (HA) and neuraminidase (NA) molecule of the different strains included in the influenza vaccine[21]. Different formulations of the trivalent influenza vaccine (TIV) are available, including the whole, split (chemically disrupted), or subunit (purified surface glycoprotein) vaccines, and generally includes the two most recent circulating strains of Influenza A and one Influenza B circulating strain. Deciding which formulation to administer is dependent on age, risk factors, and geographical location. The live attenuated influenza vaccine (LAIV) uses an attenuated cold-adapted viral backbone of the HA and NA of the target strains[18].

The response elicited by the influenza vaccine is primarily antibody mediated. Usually within two weeks, vaccine recipients have established protective antibody titers against the specific HAs and NAs of the vaccine strains[18]. Antibodies generated against the HA molecule are thought to be the major correlate of vaccine protection, whereas the NA-specific antibodies aid in reducing the severity of infection. For the TIV vaccine, the serum antibody response consists mainly of influenza-specific IgG1 antibodies, with lower but detectable amounts of IgM and IgA antibodies[22]. The split-virus TIV induces the production of antibodies that primarily target the HA and NA glycoprotein, but antibodies directed against internal viral proteins, M and NP, can also be detected. While cell-mediated responses appear to play a role in recovery from influenza infection, conclusive evidence that these responses significantly contribute to preventing infection via vaccination is still lacking. The LAIV, administered intranasally, has a

slightly lower systemic humoral response when compared to the TIV, but induces a more robust secretory response, with greater production of SIgA[22]. LAIV has been shown to produce a cellular immune response, but this hasn't been thoroughly explored.

Pandemic H1N1 was susceptible to the neuraminidase inhibitors, oseltamivir and zanamivir, but resistant to amantadine[23]. NA inhibitors prevent the virus from effectively budding from the host cell[3]. Amantadine sterically blocks the M2 channel of influenza A, preventing uncoating of the virus. Unfortunately, the therapeutic use of amantadine was discontinued in 2009 due to all circulating strains developing resistance against the drug[23]. Treatment with NA inhibitors was found to be efficacious if given within 36 hours post onset of symptoms during the pH1N1[24]. During the pandemic, the US Food and Drug Administration (FDA) issued an emergency authorization for the use of oseltamivir in infants under 1 year of age[10].

1.3   PATHOGENESIS

1.3.1   Clinical Features

Influenza typically presents with clinical signs such at fever, myalgia, malaise, headache and upper respiratory symptoms that include cough, sore throat, and rhinitis[24]. The spectrum and severity of clinical presentation varies by current health status, age, vaccination status, and is dependent on strain of virus. Pandemic H1N1 was initially considered a mild, self-limiting upper respiratory tract illness, much like that of the seasonal influenza. However, in a subset of the population, pH1N1 caused more severe pulmonary symptoms, possibly due to its receptor

tropism for 2,3-linked sialic acid linkages located in the deep respiratory tract, as opposed to seasonal influenza which typically binds to 2,6-linked sialic acid receptors in the upper respiratory tract[25].

The virus is typically spread by airborne transmission or direct contact with an infected person or animal. The incubation period is short, usually lasting only two days, followed by the abrupt onset of symptoms of an illness that typically lasts no longer than a week. A small percentage of patients develop complications from influenza infection, which include pneumonia, bronchitis, sinitus, rarely encephalitis, transverse myelitis, Reye syndrome, myocarditis and pericarditis. These complications frequently cause more than 90% of flu-related fatalities among the elderly[24].

1.3.2 Cytokines

The innate immune system is the first line of defense against invading viruses. In response to influenza infection, the innate immune system produces a pro-inflammatory and antiviral response in the form of cytokines and chemokines. Chemokines and cytokines play a major role in the pathogenesis of viral infections. Highly virulent strains of influenza viruses, such as avian H5N1 influenza, are known to cause aberrant and excessive cytokine production, resulting in higher levels of morbidity and mortality for humans and other mammals[26,27]. Increased levels of specific inflammatory cytokines, including tumor necrosis factor (TNF) α, interleukin 1 (IL-1), IL-6, IL-8, IL-12, interferon (IFN) γ, and IFN-α have been linked to disease progression and death in seasonal outbreaks of influenza[26,27]. Retrospective studies of patients severely infected with pH1N1 have identified a strong correlation with high sera levels of IL-6

and IL-10[28]. The underlying mechanism of how, or why, aberrant cytokine responses are correlated with more severe outcomes of influenza infection is unknown.

1.4   IMMUNOLOGY OF PREGNANCY

One of the most complex puzzles in modern immunology involves the "paradox of pregnancy", where the mother must simultaneously tolerate the paternal derived fetal antigens while defending the fetus and herself against infection[29]. Historically, it was thought that pregnancy was an immunologically suppressed state that led to increased infectious disease susceptibility. More recent evidence indicates that there is an immune modulatory state, where during pregnancy, the immune system responds differentially depending on a combination of factors[29]. These factors include the type of microorganism, the stage of pregnancy, the response of the fetal-placental unit, and maternal immune response.

Overall, there is evidence to suggest that the maternal immune system tolerates fetal antigens by suppressing cell-mediated immunity and maintaining humoral immunity. However, this may be an over simplification[30]. Rather than looking at the immunology of pregnancy as a singular condition, it is more prudent to consider it as three distinct phases that influence and shape the maternal immune response[29,31]. During the first phase, in the first trimester, the maternal immune system is thought to be pro-inflammatory, resulting in a T-helper type 1 (Th-1) response. The second phase, during the second trimester, is an anti-inflammatory phase that results in a T-helper type 2 (Th-2) response. During the third phase and trimester, the maternal immune system is thought to switch back to the pro-inflammatory cytokine response to promote delivery. This Th1-Th2 shift programs not only the placental-fetal response, but also the

7

systemic maternal response from an initial cell-mediated response, to a humoral response, when confronted with infection.

Adding to the complexity of the "paradox of pregnancy" is a new paradigm that proposes that the immunological response of the mother is not solely determined by the maternal response, but is also influenced by the fetal-placental unit[29]. Therefore, the immunology of pregnancy is the consequence of a combination of signals and responses from both the maternal and the fetal-placental immune system. Results from laboratory studies have suggested that the type of response initiated at the placenta might influence the immunological response of the mother. If the viral infection elicits pro-inflammatory cytokines, such as interferon (IFN gamma), interleukin 12 (IL-12), and high levels of IL-6 at the placenta, it may, in turn, overstimulate the maternal immune system and lead to adverse pregnancy outcomes[29,32]. Alternatively, if a viral infection triggers a mild inflammatory response in the placenta, it may activate the maternal immune system to protect the fetus from harm.

Consequently, pregnant women are not thought to be immunocompromised but instead experience significant immunologic changes during the course of pregnancy that may lead them to be more susceptible or more severely affected by infectious diseases. There is evidence for increased susceptibility to infectious diseases. For example, *Listeria monocytogenes,* an often invasive foodborne illness, is far more common during pregnancy, making up one third of all reported cases and resulting in a substantial amount of stillbirths[33,34]. Pregnant women are also far more likely to develop clinical signs of leprosy from *Mycobacterium leprae,* which is hypothesized to be the result of decreased cell-mediated immunity[33]. In addition to the increased susceptibility to certain infectious diseases, there is more evidence indicating that during pregnancy, there is a higher risk for developing increased disease severity. For instance, varicella

zoster infection occurring during pregnancy is more severe and can lead to varicella pneumonia[33]. It has been well documented that pregnant women experience a more severe clinical course, increased complication rates, and higher-case fatality rates during influenza pandemics[33].

As discussed above, changes in immune function over the course of pregnancy can alter a pregnant woman's susceptibility to, and severity of, certain infectious diseases. The mechanisms by which pregnant women have untoward outcomes to infectious agents have not been well explored, particularly in basic bench research. To better understand the dynamics of the immune system during pregnancy and how it modifies and interacts with infectious agents, it is essential to develop new methodologies and relevant animal models of pandemic influenza infection. This knowledge will help address challenging questions about why pregnant women are more susceptible to, or have more severe clinical outcomes to infectious diseases, how infectious agents affect the fetus and pregnancy outcome, and if there is available treatment that could benefit pregnant women.

1.5   FERRET MODEL

There are several mammalian models for studying influenza and each have their own advantages depending on the question being asked[35]. Mice are commonly used because of their low cost, readily available reagents, and the availability of transgenic mice, which allow for the study of genetic contributions. However, influenza virus does not naturally replicate in mice and therefore, the influenza strains have to be adapted. Mice also do not show similar clinical signs

and cannot transmit virus effectively, preventing the possibility of transmission and pathogenesis studies.

The ferret model is generally considered the only small mammalian model that is well-suited for the study of the pathobiology of influenza virus[35]. The ferret has been well established for the study of many respiratory viruses such as coronavirus, nipah virus and morbillivirus. The general advantages of using ferrets as an animal model are that they are relatively small and exhibit numerous clinical features associated with human disease, which is particularly true for influenza infection. This is because ferret and human lung physiology are similar, exhibiting similar distribution patterns of the 2,3- and 2,6-linked sialic acid residues which influenza uses as its entry receptor[36]. Furthermore, ferrets have similar respiratory compartments that are ideal for determining different areas of disease manifestations. Ferrets are highly susceptible to human influenza and can naturally transmit the virus to each other, making them excellent models for investigating transmission. Lastly, ferrets are well suited for vaccine efficacy and drug studies because they respond in an immunologically similar way to human infection.

We propose the use of a pregnant ferret model to investigate the immunological and virological parameters that led to the disproportionately high morbidity and mortality observed among pregnant women during the pH1N1. In the future, this pregnant ferret model could be crucial in uncovering the mechanisms as to why pregnant women have poorer clinical outcomes during influenza pandemics in comparison to the general population. It could also answer, if pH1N1 infection affects or alters the fetus and pregnancy outcome and further, could be useful in the evaluation of potential therapeutics.

2.0   STATEMENT OF THE PROJECT AND SPECIFIC AIMS

In April 2009, the World Health Organization (WHO) issued a Global Outbreak Alert as a result of laboratory confirmed human cases of Swine Influenza A/H1N1 in the USA and Mexico[37]. Two months later, the U.S. Centers for Disease Control and Prevention (CDC) and WHO declared this outbreak of swine H1N1 influenza a pandemic. Although the global infection rate was recently estimated to be 11% to 21%, much lower than previously predicted, enhanced surveillance implemented by the CDC for pregnant women in the 2009 pandemic, confirmed increased severity of infection and overall higher incidence of influenza infection among pregnant women[16]. These results are consistent with what has been observed in previous influenza pandemics and seasonal epidemics.

There has been little examination of the exact mechanism that is responsible for this disproportionate morbidity and mortality. It is believed that pregnancy creates an immune modulatory state to prevent rejection of the fetus, but additional investigation of the contribution of this condition in the pathogenesis of viruses has not been thoroughly explored[30]. To this end, a pregnant animal model for pH1N1 is necessary to investigate the immunological parameters of this disparity and to be able to evaluate possible interventions in the future.

The ferret model has been well established for the study of influenza virus and has been proven to be a good model for studying various aspects of the human disease compared to the mouse model[35]. This is because influenza infection closely resembles that in humans with similar

characteristics of clinical signs, pathogenesis and immunity. Also, ferrets are considered a natural host for both Type A and B human influenza viruses so strains do not need to be adapted. Furthermore, ferrets have other physical characteristics that are similar to humans, such as a long trachea and differing respiratory compartments, which are ideal for determining different areas of disease manifestation.

In the last two years, the Stefano-Cole laboratory has worked to develop a pregnant ferret model for pandemic 2009 H1N1 using an aerosol challenge method. Timed-pregnant ferrets were received at 27d of a 42d gestational period, and exposed to aerosolized H1N1 on d32 to simulate the third trimester of pregnancy in humans. Following infection, all ferrets were monitored for clinical signs of disease and tissues were harvested at necropsy for further histological and immunological analyses.

2.1   HYPOTHESIS

Increased morbidity and mortality has been reported among pregnant women for both pandemic and seasonal epidemics of influenza. However, little is known about the mechanism(s) responsible for this disproportionate morbidity and mortality. We have established a pregnant ferret model for evaluation of 2009 H1N1 influenza infection during late stage pregnancy. The goal of this project is to evaluate clinical, viral and immunologic parameters associated with increased morbidity and mortality in pregnant ferrets infected with aerosolized H1N1. *Our working hypothesis was that increased morbidity and mortality observed with H1N1 infection during late stage pregnancy is due to differences in early immune responses rather than quantitative levels of virus replication and dissemination.*

2.1.1   Specific Aim 1: To compare quantitative viral loads and viral dissemination between pregnant and non-pregnant ferrets.

To compare quantitative viral loads and tissue dissemination between pregnant and non-pregnant ferrets we used quantitative reverse transcriptase real-time polymerase chain reaction (rRT-PCR) to detect viral copies in lung, spleen, liver, brain, fetal brain, fetus, placenta, uterus, and plasma. Also, our pathologist (T.D.O.), characterized pathological changes associated with H1N1 infection from the tissues harvested at necropsy.

2.1.2   Specific Aim 2: To elucidate differences in innate immunity elicited by H1N1 infection in pregnant and non-pregnant ferrets.

To obtain mRNA levels in lung, spleen, placenta, uterus and fetus we used semi-quantitative real-time polymerase chain reaction (RT-PCR) to detect interferon-α (IFN-α), interferon-γ (IFN-γ), tumor necrosis factor-α (TNF-α), interleukin-6 (IL-6), interleukin-10 (IL-10), interleukin-12p40 (IL-12p40), and glyceraldehyde 3-phosphate dehydrogenase (GAPDH). To calculate the fold change we used the ($\Delta\Delta$Cycle threshold $\Delta\Delta$Ct) method by standardizing to GAPDH levels and comparing back to baseline (Day 0) levels. We also, monitored the development of antibody responses over the course infection by hemagglutination inhibition assay (HAI).

3.0   METHODS AND MATERIALS

3.1   FERRET STUDY

Eight of each 2009 H1N1 sero-negative, timed pregnant (received on day 27 of an approximate 42 day gestation) and control (non-pregnant) ferrets were received from Triple F Farms (Sayre, PA). Ferrets were housed in ABSL-2 containment for the duration of the study. Research was conducted at the University of Pittsburgh and was in compliance with the Animal Welfare Act and other federal statutes and regulations relating to animals and experiments involving animals. The University of Pittsburgh is fully accredited by the Association for Assessment and Accreditation of Laboratory Animal Care International.

All ferrets rested for 24 hours after transport prior to subcutaneous implantation of IPTT-300 temperature chips (BioMedic Data Systems, Seaford, DE).   Ferrets were allowed to acclimate for an additional 4 days prior to challenge with aerosolized 2009 H1N1. Immediately following challenge (day 0), two each non-pregnant (control) and pregnant ferrets were sacrificed and tissues were harvested for subsequent pathologic and virologic analysis. On days 3, 5, and 7 post-challenge, two ferrets in each the control and pregnant cohorts were again sacrificed to monitor the progression of infection in vivo (Table 1). All ferrets were monitored daily for weights and body temperatures prior to and after infectious challenge. Clinical signs of infection that included lethargy, reduced food and water intake, changes in behavior, nasal

discharge, sneezing, labored breathing and spontaneous premature delivery were also observed. Ferrets that became moribund (defined as >25% weight loss, clinical signs or combination of both) were euthanized promptly. All harvested tissues were flash frozen in liquid nitrogen or stored in 2% formalin at -80°C.

Table 1. Ferret Serial Sacrifice Study

Pregnant		Non-pregnant	
ID Number	**Day Sacrificed**	**ID Number**	**Day Sacrificed**
97-11	0	112-11	0
100-11	0	107-11	0
98-11	3	105-11	3
103-11	3	110-11	3
99-11	5	111-11	5
102-11	5	108-11	5
101-11	7	106-11	7
104-11	7	109-11	7

3.2   VIRUS PROPAGATION AND INNCOLATION INTO FERRETS

3.2.1   Virus

A high titer stock of 2009 H1N1 influenza (A/California/04/09) was grown in MDCK cells using the procedure described in the Appendix and frozen at $^-80^oC$ until use. Titer was confirmed by incubation with MDCK cells to evaluate cytopathic effect in a $TCID_{50}$ assay using the Reed-Muench formula[38] and confirmed by hemagglutination with turkey erythrocytes (Lampire Biologicals).

3.2.2   Aerosol challenge

Aerosols containing influenza virus were generated using a Collison 3-jet nebulizer (BGI®, Waltham, MA) controlled by the AeroMP system (Biaera Technologies, Hagerstown, MD) inside a class III biological safety cabinet (Baker Co., Sanford, ME). Ferrets were exposed in groups of 4 (two pregnant, two control ferrets) for 10 minutes to aerosolized influenza virus in a whole-body exposure chamber (Biaera Technologies). Presented dose was determined from aerosol samples collected in an all-glass impinger (AGI) containing 10 ml of DMEM and 0.5% BSA. Using Guyton's formula for respiratory minute volume, the presented dose was estimated to be 1504 ± 339 TCID$_{50}$ of pH1N1.

3.3   QUANTITATIVE REVERSE TRANSCRIPTASE REAL TIME POLYMERASE CHAIN REACTION (rRT-PCR)

3.3.1   RNA Extraction and Primer Design

Lung, liver, spleen, placenta, uterus, fetus, brain and plasma of 2 ferrets per group (pregnant and no pregnant) were harvested at 0, 3, 5 and 7 days post infection (D.P.I.). Tissue homogenates and plasma were used for PCR analysis. From each tissue 100mg was homogenized and RNA extracted using TRI Reagent (Ambien, Grand Island, NY). Following the manufactures guidelines RNA was further purified using the MagMAX-96 for Microarrays Kit (Ambion, Grand Island, NY) by the spin procedure. One-step quantitative real-time reverse transcription-PCR was performed following the protocol established by the WHO Collaborating

Centre for influenza using the Invitrogen Superscript III Platinum One-Step Quantitative Kit (Invitrogen, Carlsbad, CA) based on the detection of the H1N1 matrix and nucleoprotein gene listed in Appendix Table 3 (Biosearch Technologies, Inc., Novato, CA)[39]. Controls and a standard curve (series of twofold dilutions starting with 3 x 10^6 A/California/04/09) were included from viral stocks and day 0 tissue samples. Standard curve cycle threshold (CT) values began at ~16 for both primer sets and each dilution was ~ 2.5 cycle thresholds above the next.

3.3.2 PCR

Samples were analyzed by real-time PCR with a 7900HT Fast Real-Time PCR system (Applied Biosystems, Carlsbad, CA) for 40 cycles using the PCR reagents listed in Table 4. When all controls met the expected results, the sample was considered positive for pH1N1 if both reaction growth curves crossed the threshold line within 40 cycles using a thermocycler program listed in Table 5.

3.4   HISTOLOGICAL ANALYSIS

All tissues were harvested immediately following sacrifice of each animal, and preserved in 2% formalin at -80°C. Six micron thick sections of tissues were stained with hematoxylin and eosin and evaluated for pathology by a board certified anatomic pathologist (T.D.O).

3.5   QUANTIFICATION OF MRNA

3.5.1   RNA Extraction, cDNA synthesis and Primer Design

RNA isolation was performed on ferret lungs, spleen, fetus, placenta and uterus using the RNeasy Mini Kit and on-column DNase digestion protocols (Qiagen). First strand cDNA synthesis was performed using 0.5µg RNA and Maxima First Strand cDNA Synthesis kit (Thermo Scientific, Hanover Park, IL). Primer sequences for interferon (IFN) γ, IFN-α, tumor necrosis factor (TNF) α interleukin (IL) 6, IL-10, IL-12p40 and GAPDH (Integrated DNA Technologies, Coralville, IA) were published elsewhere[40,41] and are listed in Appendix Table 6.

3.5.2   PCR

Semiquantitative reverse-transcription polymerase chain reaction was performed using 0.5µg of RNA, Maxima SYBR Green qPCR Master Mix (Thermo Scientific, Hanover Park, IL) and an Bio-Rad MiniOpticon using the protocol listed in Table 7 and Gene Expression program in Table 8. Expression levels were normalized to Glyceraldehyde-3-Phosphate Dehydrogenase (GAPDH) and are reported as fold change compared with day 0 animals based on the ΔΔCt method. To obtain the ΔCt, GAPDH Ct value was subtracted from the gene of interest at each time point. The fold change was calculated by subtracting the day 0 ΔCt values from the subsequent days ΔCt values. To obtain these values as absolute values, the formula, fold change $= 2^{-\Delta\Delta CT}$ was used[42].

3.6   SEROLOGICAL ANALYSIS

Whole blood samples collected from each ferret were processed to sera by allowing clot formation at room temperature for 30 minutes followed by clot removal by centrifugation at 1,000 x g for 10 minutes at 4°C. Serum was further absorbed using 0.5% Turkey red blood cells (TRBCs) (Lampire Biological Labs, Pipersville, PA) and heat inactivated at 57℃ for 30 minutes. A hemagglutination inhibition assay (HAI) was used to determine antibody titers using 1% TRBCs. HAI assay detects the serum antibodies to the viral hemagglutinin by measuring the inhibition of virus-mediated agglutination of turkey erthyocytes. Briefly, TRBCs were washed with 1X PBS and resuspended to a final concentration of 1% TRBCs/volume. In 96 vee-bottom plates, serum was first serially diluted (twofold) in the plate in duplicate columns. Virus was diluted to contain four agglutinating units in sterile PBS and added to all wells except for the negative control column. Plates were then incubated for 30 minutes and agglutination was observed. Nonagglutinating cells are defined as having all cells drop to the bottom forming a button whereas agglutinating cells didn't settle to the bottom but instead formed a lattice. The HAI titer of the serum sample was determined to be the last dilution where cells were not agglutinated.

4.0   RESULTS

Sixteen influenza sero-negative age-matched control ferrets and timed-pregnant ferrets were received on day 27 of a 42-day gestational period. Both ferret groups were allowed to acclimate for 5 days and then aerosol challenged with pandemic H1N1. The timed-pregnant ferret group was challenged on gestational day 32 to stimulate beginning of third trimester for the pregnant ferrets. Two ferrets from each group were serially sacrificed and tissues were taken on day 0 (immediately post-infection), day 3, day 5 and day 7. Temperature, weight and clinical signs were monitored prior to and throughout infection.

4.1   CLINICAL MONITORING POST INFECTION

Temperature in both groups, pregnant and non-pregnant peaked at 1-2 days post infection (D.P.I.) and subsequently returned to the normal range by day 3 PI (Figure 1A). The pregnant ferret group displayed greater weight loss continuously over the course of infection compared to the non-pregnant ferret group that returned to baseline weight by day 3 PI (Figure 1B). Weight loss continuously throughout infection in the pregnant ferret group is particularly alarming because the start of the 3rd trimester is typically when the most weight is gained. The pregnant ferret group also displayed more severe clinical signs compared to the non-pregnant infected

20

ferret group such as greater lethargy, reduced food and water intake, nasal discharge with sneezing, as well as labored breathing by day 3-7 PI (Figure 1C).
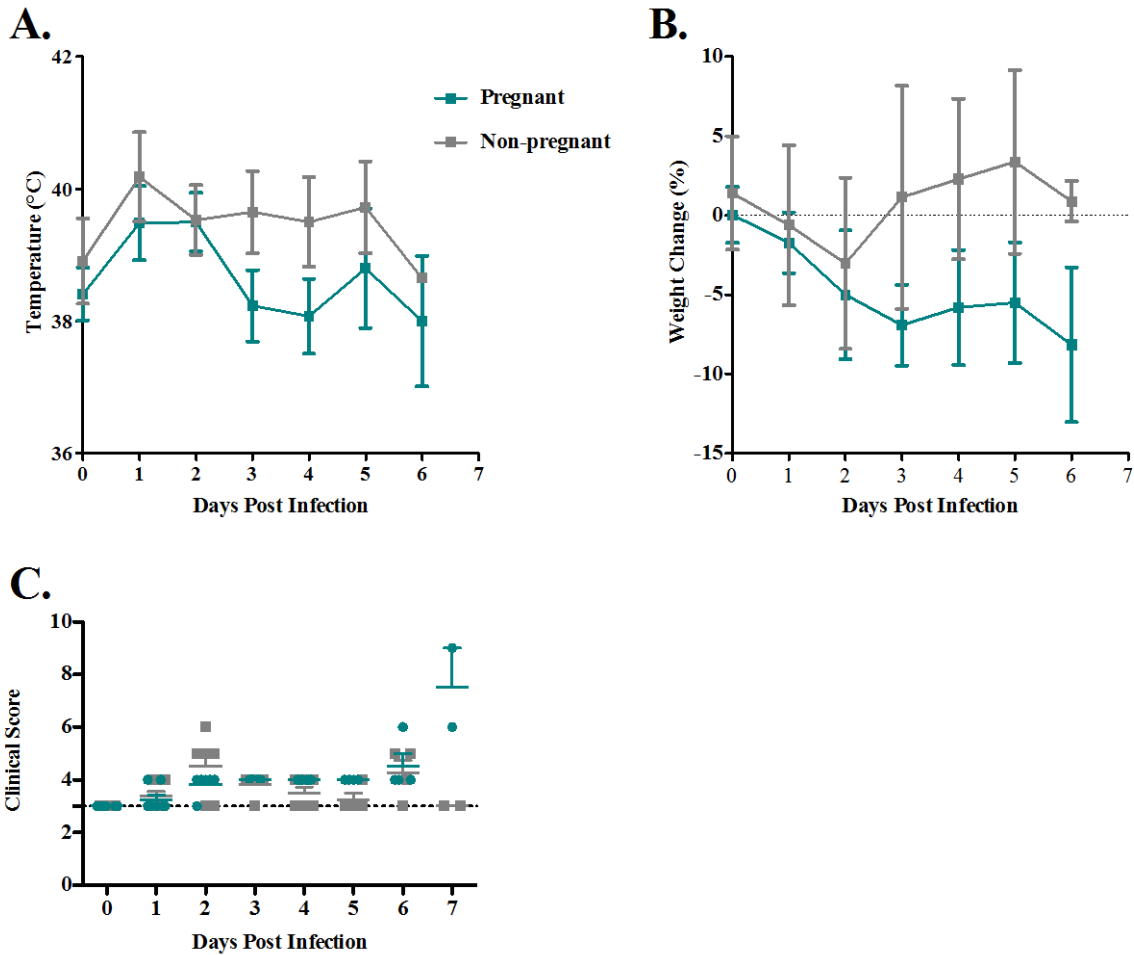
Figure 1. Clinical signs of non-pregnant and pregnant ferrets after aerosol exposure to A/California/04/09 during serial sacrifice study.

Eight pregnant ferrets at day 33 gestation and eight non-pregnant ferrets were aerosol exposed to 1.75×10^4 pfu A/California/04/09. Two ferrets from each group were serially sacrificed on day 0 (immediately after exposure), day 3, day 5 and day 7. **(A)** Temperature change of pregnant and non-pregnant ferrets over the course of infection. **(B)** Percentage weight change of pregnant and non-pregnant ferrets over the course of infection. **(C)** Clinical Score based on each ferrets behavior, appearance, temperature and weight change over the course of infection. Means are shown with standard deviation (SD) for each time point.

4.2 SPECIFIC AIM 1: TO COMPARE QUANTITATIVE VIRAL LOADS AND VIRAL DISSEMINATION BETWEEN PREGNANT AND NON-PREGNANT FERRETS

4.2.1 Viral Dissemination and Load

To test whether differences in dissemination and/or viral load contributed to the more severe clinical outcomes in the pregnant ferret group compared to the non-pregnant group we used semi-quantitative reverse transcriptase RT-PCR to detect viral copy levels in tissues. Tissues tested included lung, brain, placenta, uterus, fetus, spleen, liver, heart and fetal brain. Data will be displayed in two forms, in panel A by dot plot and panel B a box plot. Formal statistics were not possible due to n=2 at each time point but standard deviation is shown.

4.2.1.1 Lung

Viral copies were detected at similar levels immediately post challenge in both the pregnant and non-pregnant ferret group (Figure 2). In the lung, viral copies peaked at day 3 PI and gradually decreased on day 5 and 7 PI in both pregnant and non-pregnant groups.

Figure 2. Tissue dissemination and viral loads in lungs of pregnant and non-pregnant ferrets infected with A/California/04/09.

Two ferrets from each of the pregnant and non-pregnant groups on day 0, 3, 5, and 7 were sacrificed. Samples of lung were used for RNA isolation to determine viral load by quantitative rRT-PCR. Viral copies were determined by the standard curve method using two separate primers (universal InfA primer and swine InfA primer). **(A)** Viral copies determined in lung homogenates of each primer set in pregnant (grey dots) and non-pregnant ferrets (black dots) shown as a dot plot with mean and SD. **(B)** Viral copies determined in lung of each ferret group shown as a box and whiskers plot with mean and SD.

4.2.1.2 Brain

Virus was also detected in the brains of most ferrets by day 3 PI and remained at a continuous level for the duration of the study in both pregnant and non-pregnant ferret groups (Figure 3). One of two ferrets in the non-pregnant group on days 5 and 7 PI were negative for both primer sets against pH1N1. This result indicates that aerosol challenge of pH1N1 is able to progress up the olfactory bulb or possible disseminate through central nervous system.

Figure 3. Tissue dissemination and viral loads in brains of pregnant and non-pregnant ferrets infected with A/California/04/09.

Two ferrets from each of the pregnant and non-pregnant groups on day 0, 3, 5, and 7 were sacrificed. Samples of brain were used for RNA isolation to determine viral load by quantitative rRT-PCR. Viral copies were determined by the standard curve method using two separate primers (universal InfA primer and swine InfA primer). **(A)** Viral copies determined in brains homogenates of each primer set in pregnant (grey dots) and non-pregnant ferrets (black dots) shown as a dot plot with mean and SD. **(B)** Viral copies determined in brains of each ferret group shown as a box and whiskers plot with mean and SD.

24

4.2.1.3 Placenta and Uterus

Low levels of pH1N1 viral copies were detected in the placenta of the pregnant ferrets by day 3 PI and consistently found throughout the course of infection (Figure 4). No viral copies were found in the uterus tissue of non-pregnant ferret groups.
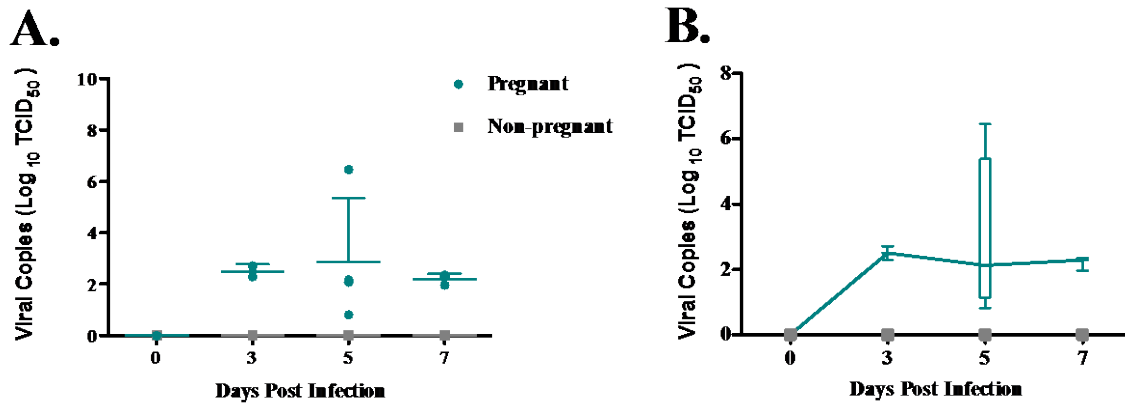
Figure 4. Tissue dissemination and viral loads in placentas of pregnant and uteruses of non-pregnant ferrets infected with A/California/04/09.

Two ferrets from each of the pregnant and non-pregnant groups on day 0, 3, 5, and 7 were sacrificed. Samples of placentas and uteruses were used for RNA isolation to determine viral load by quantitative rRT-PCR. Viral copies were determined by the standard curve method using two separate primers (universal InfA primer and swine InfA primer). **(A)** Viral copies determined in placenta and uterus homogenates of each primer set in pregnant (grey dots) and non-pregnant ferrets (black dots) shown as a dot plot with mean and SD. **(B)** Viral copies determined in placenta and uterus of each ferret group shown as a box and whiskers plot with mean and SD.

4.2.1.4 Fetus

Quantifiable pH1N1 viral copies were detected in the fetus of both pregnant ferrets at day 7 PI at low levels (Figure 5). Fetal brain was also tested for viral presence but no detectable levels of pH1N1 were present.
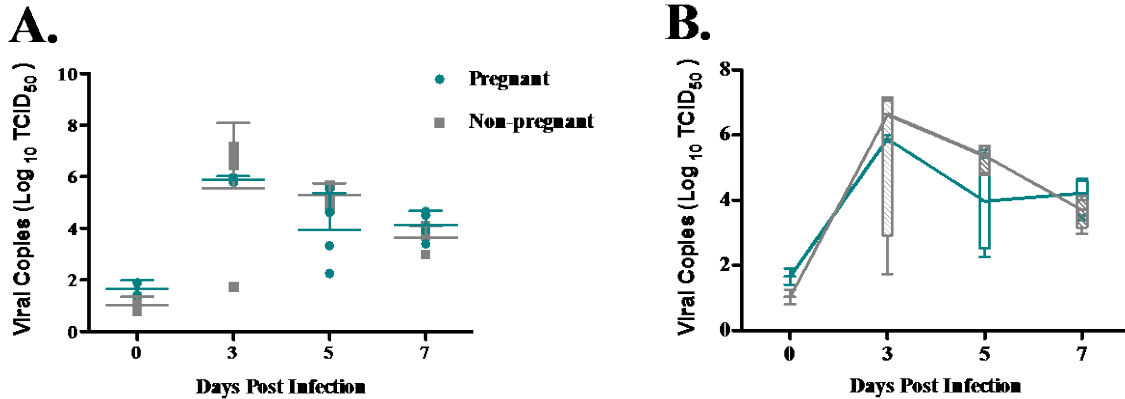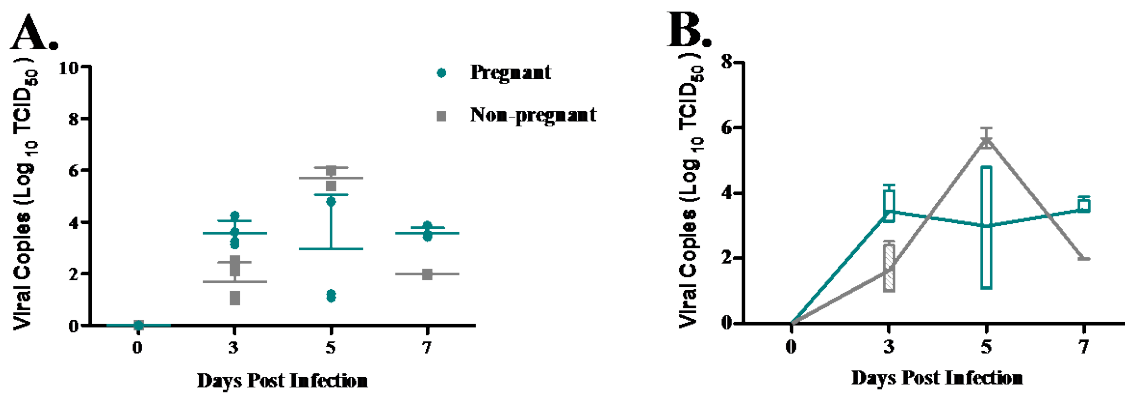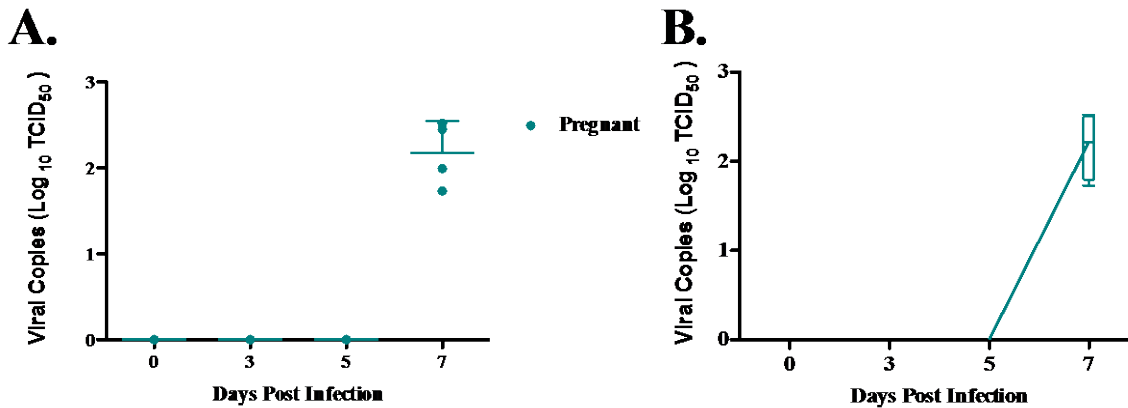

Figure 5. Tissue dissemination and viral loads in fetus of pregnant and non-pregnant ferrets infected with A/California/04/09.

Two ferrets from each of the pregnant and non-pregnant groups on day 0, 3, 5, and 7 were sacrificed. Samples of fetal tissue were used for RNA isolation to determine viral load by quantitative rRT-PCR. Viral copies were determined by the standard curve method using two separate primers (universal InfA primer and swine InfA primer). **(A)** Viral copies determined in fetal homogenates of each primer set of pregnant (grey dots) shown as a dot plot with mean and SD. **(B)** Viral copies determined in fetus of each ferret group shown as a box and whiskers plot with mean and SD.

4.2.2 Pathology

Histologic analyses of tissues sections from the ferrets revealed that most pathologic changes were observed in the lung (Figure 6). Lungs in both pregnant and non-pregnant groups had fluctuating levels of pulmonary alveolar proteinosis at different time points (Table 2). Beginning at day 3 PI and extending throughout infection in both the pregnant and non-pregnant ferrets groups displayed larger bronchi and an accumulation of foamy macrophages (Figure 6). By day 5 and 7 PI the larger airways became plugged with necrotic debris, residual inflammatory cells, peri-bronchial and perivascular lymphatic inflammation. A summary of the pulmonary changes is shown in Table 2. No obvious pathologic changes were distinguishable between the pregnant and non-pregnant ferret groups.

Figure 6. Histologic images of lung sections showing prominent pathologic responses after aerosol infection with H1N1 2009 influenza.

(A) Lung section from non-pregnant ferret at day 0 showing areas of normal alveoli (upper left) adjacent to alveolar spaces filled with proteinaceous material (alveolar proteinosis, lower right). Lung section from a pregnant ferret 7 days after infection showing diffuse pulmonary alveolar proteinosis **(B)**, large airway plugging with mucus and inflammatory cells **(C),** and a bronchial with peribronchial inflammation and plugging with inflammation and necrotic debris **(D).**

Table 2. Pathologic changes noted in the lungs of pregnant and non-pregnant ferrets at various time points (days) after infection with influenza virus.

Pathology	Group	Day 0	Day 3	Day 5	Day 7
PAP	Pregnant	1/2	2/2	2/2	2/2
	Non-pregnant	2/2	0/2	2/2	1/2
Large airway plugging/foamy macrophages	Pregnant	0/2	2/2	2/2	2/2
	Non-pregnant	0/2	2/2	2/2	2/2
Peri-bronchial and peri-vascular inflammation	Pregnant	0/2	2/2	2/2	2/2
	Non-pregnant	0/2	0/2	1/2	2/2

Pathologic changes include pulmonary alveolar proteinosis (PAP), plugging of large airways with necrotic debris or foamy macrophages, and peri-bronchial and peri-vascular lymphocytic inflammation. Values represent number of ferrets with pathology in indicated organ at dose of virus per number of ferrets in the treatment group.

No pathologic changes were observed in the liver, heart, spleen, brain, or fetus at any time point. No obvious pathology was seen in the placenta, but there may have been a mild increase in villi epithelial cell apoptosis at days 5 and 7 post viral exposure (Figure 7).
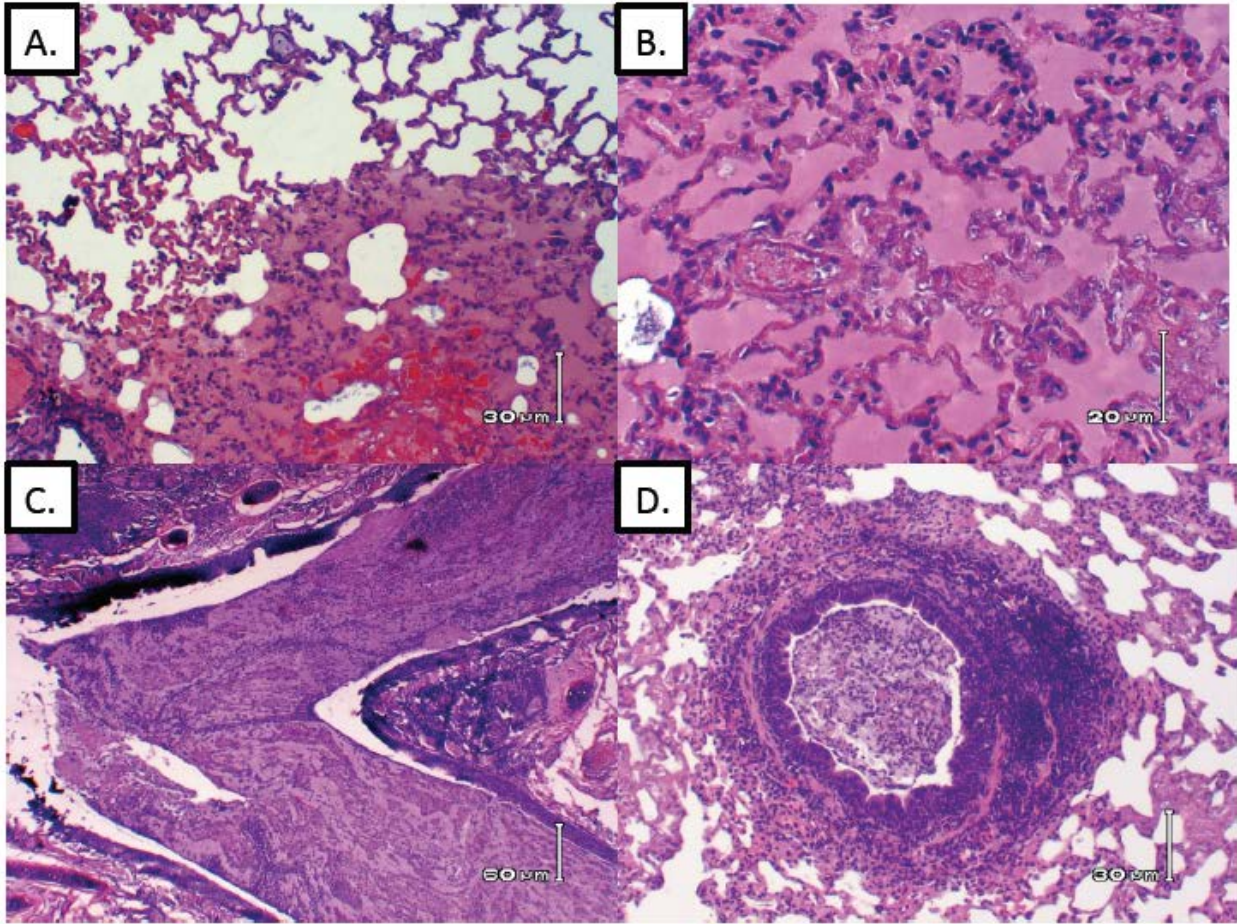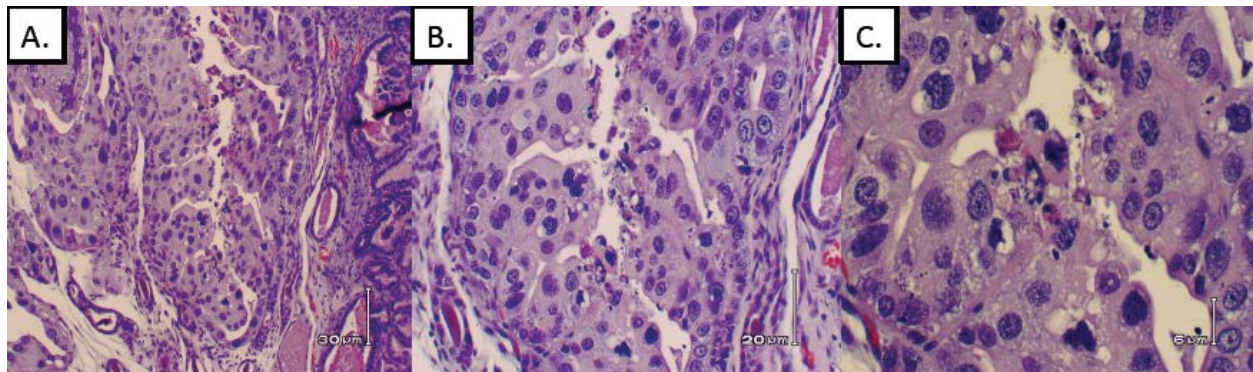

Figure 7. Histologic images of placenta sections showing pathologic responses after aerosol infection with H1N1 2009 influenza.

(A) Placenta section from pregnant ferret at day 7 showing areas of normal placenta architecture and increased magnification on areas of apoptotic bodies (B and C).

4.2.3 Summary of Aim 1

In summary, pregnant ferrets demonstrated an increased severity of clinical disease highlighted by a greater weight loss and more severe clinical signs relative to non-pregnant ferrets. Disease severity in the pregnant ferrets was not due to discernable differences in viral dissemination or greater viral burden. In addition, pulmonary pathology observed in both pregnant and non-pregnant ferrets was comparable. Viral copies detected in the placenta by 3 DPI and fetus by 7 DPI suggests possible fetal transmission. Placental pathology included a mild increase in villi epithelial cell apoptosis by 5 DPI, the relevance of which in unknown at this time.

4.3   SPECIFIC AIM 2: TO ELUCIDATE DIFFERENCES IN INNATE IMMUNITY ELICITED BY H1N1 INFECTION IN PREGNANT AND NON-PREGNANT FERRETS

4.3.1   mRNA Transcript Levels of Innate Immune Response

Pregnancy is an immune modulatory state in which host immune response is dampened and skewed toward a Th2 response[29]. To test whether differences in mRNA transcript levels of innate immune response genes contributed to the more severe clinical outcomes in the pregnant ferret group compared to the non-pregnant group, semi-quantitative RT-PCR using the housekeeping gene, GAPDH to quantify transcript levels of interferon (IFN) γ, IFN-α, tumor necrosis factor (TNF) α, interleukin (IL) 6, IL-10, and IL-12p40 was used. Tissues tested included lung, spleen, placenta, uterus, and fetus.

Due to initial discrepancies in basal levels of cytokines in the pregnant compared to the non-pregnant ferret groups, the following cytokine mRNA levels were graphed using two reference groups, we have (a) compared back to each group's own day 0 reference levels and (b) compared both groups back to non-pregnant day 0 to reveal basal cytokine transcript differences.

4.3.1.1 Lung

Pregnant ferrets had lower initial basal levels in lung tissue of IL-6, IFN-γ and IL-10 but greater initial levels of IFN-α and TNF-α (Figure 8). Upon infection, pregnant ferrets had elevated levels of IL-6, IFN-γ, TNF-α and IL-10 by day 3 and 5 PI compared to the non-pregnant ferrets suggesting a heightened pro-inflammatory response. Initial levels of IFN-α and TNF- α were higher in the pregnant ferret lungs and peak at day 5 PI before decreasing.

Lung

A.

IL-6

B.

IL-6

C.

IFN-α

D.

IFN-α

E.

IFN-γ

F.

IFN-γ

G.

TNF-α

H.

TNF-α

I.

IL-10

J.

IL-10

Figure 8. Cytokine levels in lung tissue of pregnant and non-pregnant ferrets infected with A/California/04/09.

Two ferrets from each of the pregnant and non-pregnant groups on day 0, 3, 5, and 7 were sacrificed. Lung samples were assessed for cytokine messenger RNA expression (n=2 per time point) using RT-PCR and are represented as the mean fold change shown with standard deviation compared to the values of their own reference group (a) and (b) compared to the day 0 non-pregnant ferret group. **(A)** Interleukin 6 (IL-6) mRNA levels in the lung homogenates of pregnant and non-pregnant ferrets compared back to their own group day 0 time point. **(B)** IL-6 mRNA levels in the lung homogenates of pregnant and non- pregnant ferrets compared back to the non-pregnant day 0 time point. **(C)** Interferon α (IFN-α) mRNA levels in the lung homogenates of pregnant and non-pregnant ferrets compared back to their own group day 0 time point. **(D)** IFN-α mRNA levels in the lung homogenates of pregnant and non-pregnant ferrets compared back to the non-pregnant day 0 time point. **(E)** Interferon γ (IFN-γ) mRNA levels in the lung homogenates of pregnant and non-pregnant ferrets compared back to their own group day 0 time point. **(F)** IFN-γ mRNA levels in the lung homogenates of pregnant and non-pregnant ferrets compared back to the non-pregnant day 0 time point. **(G)** Tumor necrosis factor α (TNF-α) mRNA levels in the lung homogenates of pregnant and non-pregnant ferrets compared back to their own group day 0 time point. **(H)** TNF-α mRNA levels in the lung homogenates of pregnant and non-pregnant ferrets compared back to the non-pregnant day 0 time point. **(I)** Interleukin 10 (IL-10) mRNA levels in the lung homogenates of pregnant and non-pregnant ferrets compared back to their own group day 0 time point. **(J)** IL-10 mRNA levels in the lung homogenates of pregnant and non-pregnant ferrets compared back to the non-pregnant day 0 time point.

4.3.1.2 Spleen

Pregnant ferrets had lower initial basal levels of IL-6, IFN-γ, and IL-12p40 but elevated initial levels of IFN-α and IL-10 in spleen tissue compared to non-pregnant day 0 levels (Figure 9). IL-6, IFN-γ and IL-12p40 levels in the pregnant ferrets dramatically increased compared to pregnant day 0 by day 3 PI levels but were not elevated compared back to the non-pregnant day 0 reference group. IFN-α levels in pregnant ferrets had high initial levels in the spleen compared to the non-pregnant day 0 group but decreased upon infection. IFN-α levels peaked in spleen of the non-pregnant ferrets at day 5 PI and subsequently decreased. IL-10 levels in the spleen of pregnant ferrets were initially high compared to the non-pregnant reference group but decreased steadily over the course of infection whereas the non-pregnant ferret group increased over the course of infection peaking at day 7 PI.
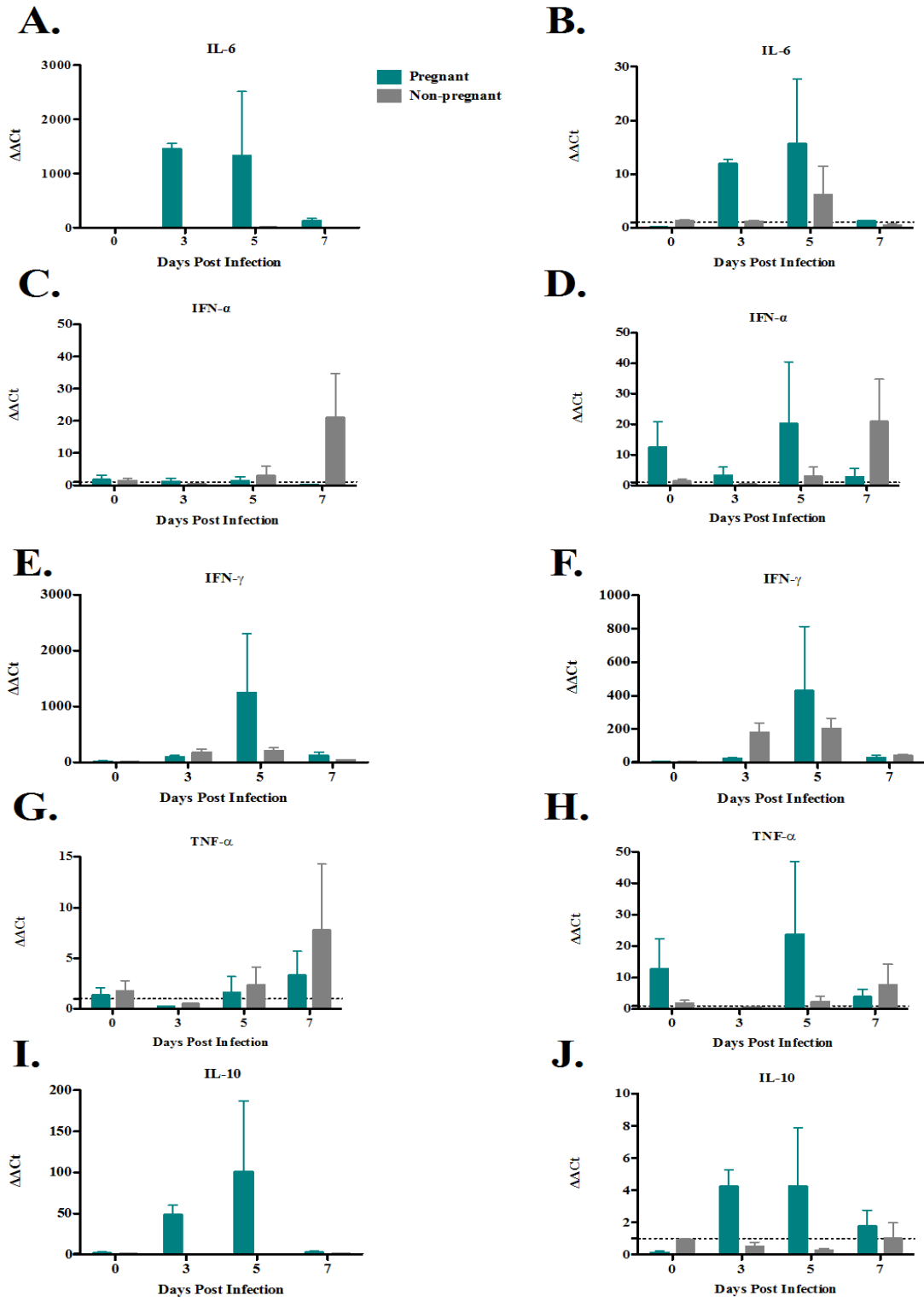
Spleen
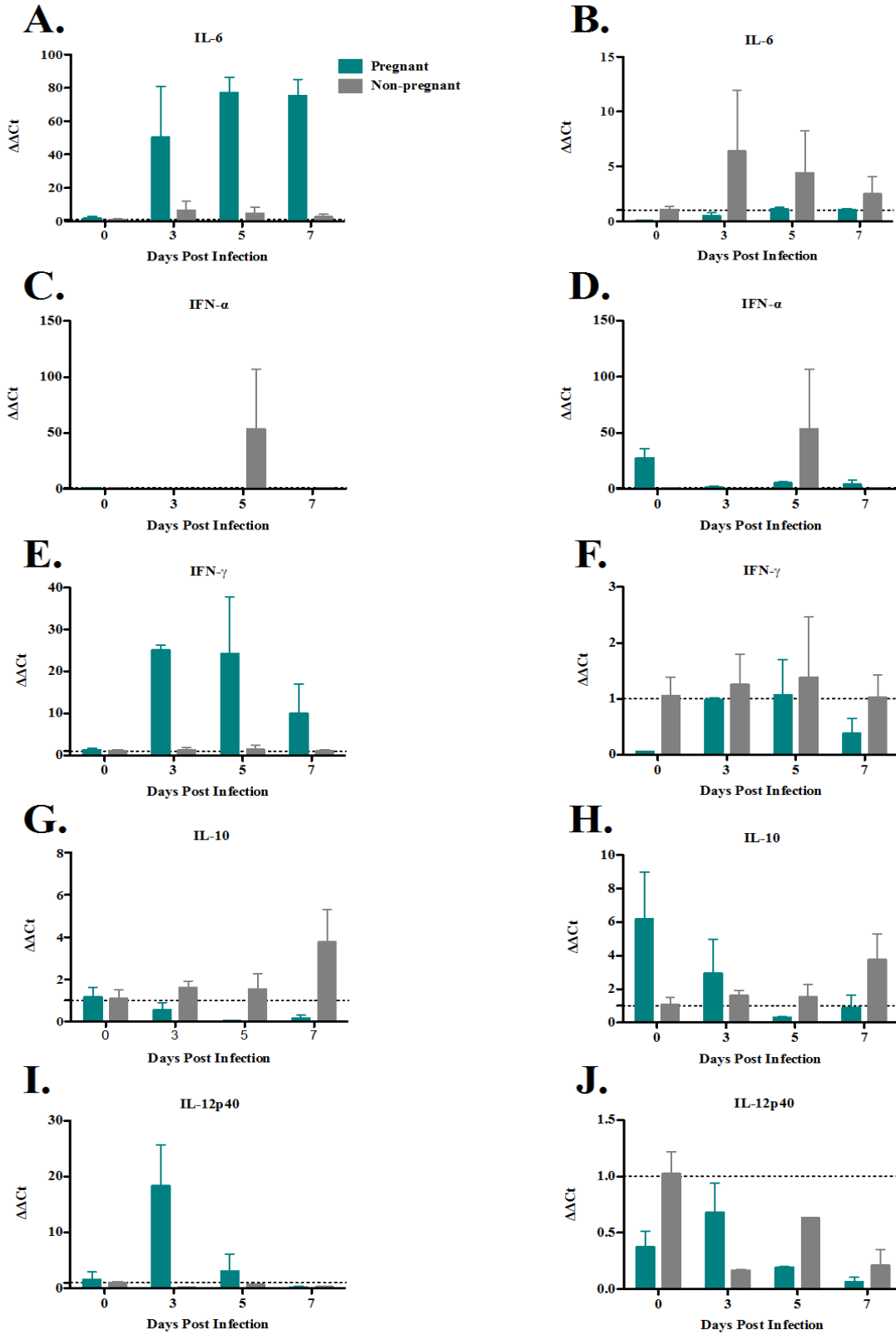
Figure 9. Cytokine levels in spleen tissue of pregnant and non-pregnant ferrets infected with A/California/04/09.

Two ferrets from each of the pregnant and non-pregnant groups on day 0, 3, 5, and 7 were sacrificed. Spleen samples were assessed for cytokine messenger RNA expression (n=2 per time point) using RT-PCR and are represented as the mean fold change (standard deviation) compared to the values of their own reference group (a) and (b) compared to the day 0 non-pregnant ferret group. **(A)** Interleukin 6 (IL-6) mRNA levels in the spleen homogenates of pregnant and non-pregnant ferrets compared back to their own group day 0 time point. **(B)** IL-6 mRNA levels in the spleen homogenates of pregnant and non- pregnant ferrets compared back to the non-pregnant day 0 time point. **(C)** Interferon α (IFN-α) mRNA levels in the spleen homogenates of pregnant and non-pregnant ferrets compared back to their own group day 0 time point. **(D)** IFN-α mRNA levels in the spleen homogenates of pregnant and non-pregnant ferrets compared back to the non-pregnant day 0 time point. **(E)** Interferon γ (IFN-γ) mRNA levels in the spleen homogenates of pregnant and non-pregnant ferrets compared back to their own group day 0 time point. **(F)** IFN-γ mRNA levels in the spleen homogenates of pregnant and non-pregnant ferrets compared back to the non-pregnant day 0 time point. **(G)** Interleukin 10 (IL-10) mRNA levels in the spleen homogenates of pregnant and non-pregnant ferrets compared back to their own group day 0 time point. **(H)** IL-10 mRNA levels in the spleen homogenates of pregnant and non-pregnant ferrets compared back to the non-pregnant day 0 time point. **(I)** Interleukin 12p40 (IL-12p40) mRNA levels in the spleen homogenates of pregnant and non-pregnant ferrets compared back to their own group day 0 time point. **(J)** IL-12p40 mRNA levels in the spleen homogenates of pregnant and non-pregnant ferrets compared back to the non-pregnant day 0 time point.

4.3.1.3 Placenta and Uterus

Initially, pregnant ferret placentas had similar levels of IL-6, IFN-γ and IL-12p40, elevated levels of IL-10 and lower levels of IFN-α compared to the non-pregnant day 0 uteruses (Figure 10). IL-6 levels peaked in the placenta of the pregnant ferrets at day 3 PI and subsequently decreased back to initial levels but no change was observed in the uterus of the non-pregnant ferrets over the course of infection. IFN-α and IFN-γ mRNA levels peaked by day 3 PI in the placenta however compared to the uterus levels did not significantly increase. IL-10 mRNA levels in the placenta of pregnant ferrets were initially high compared to the non-pregnant reference group and peaked at day 3 PI. IL-12p40 mRNA levels were not significantly different between the two groups and did not dramatically change over the course of infection.

Placenta and Uterus

A. IL-6 — ΔΔCt vs Days Post Infection (Pregnant placenta, Non-pregnant uterus)

B. IL-6 — ΔΔCt vs Days Post Infection

C. IFN-α — ΔΔCt vs Days Post Infection

D. IFN-α — ΔΔCt vs Days Post Infection

E. IFN-γ — ΔΔCt vs Days Post Infection

F. IFN-γ — ΔΔCt vs Days Post Infection

G. IL-10 — ΔΔCt vs Days Post Infection

H. IL-10 — ΔΔCt vs Days Post Infection

I. IL-12p40 — ΔΔCt vs Days Post Infection

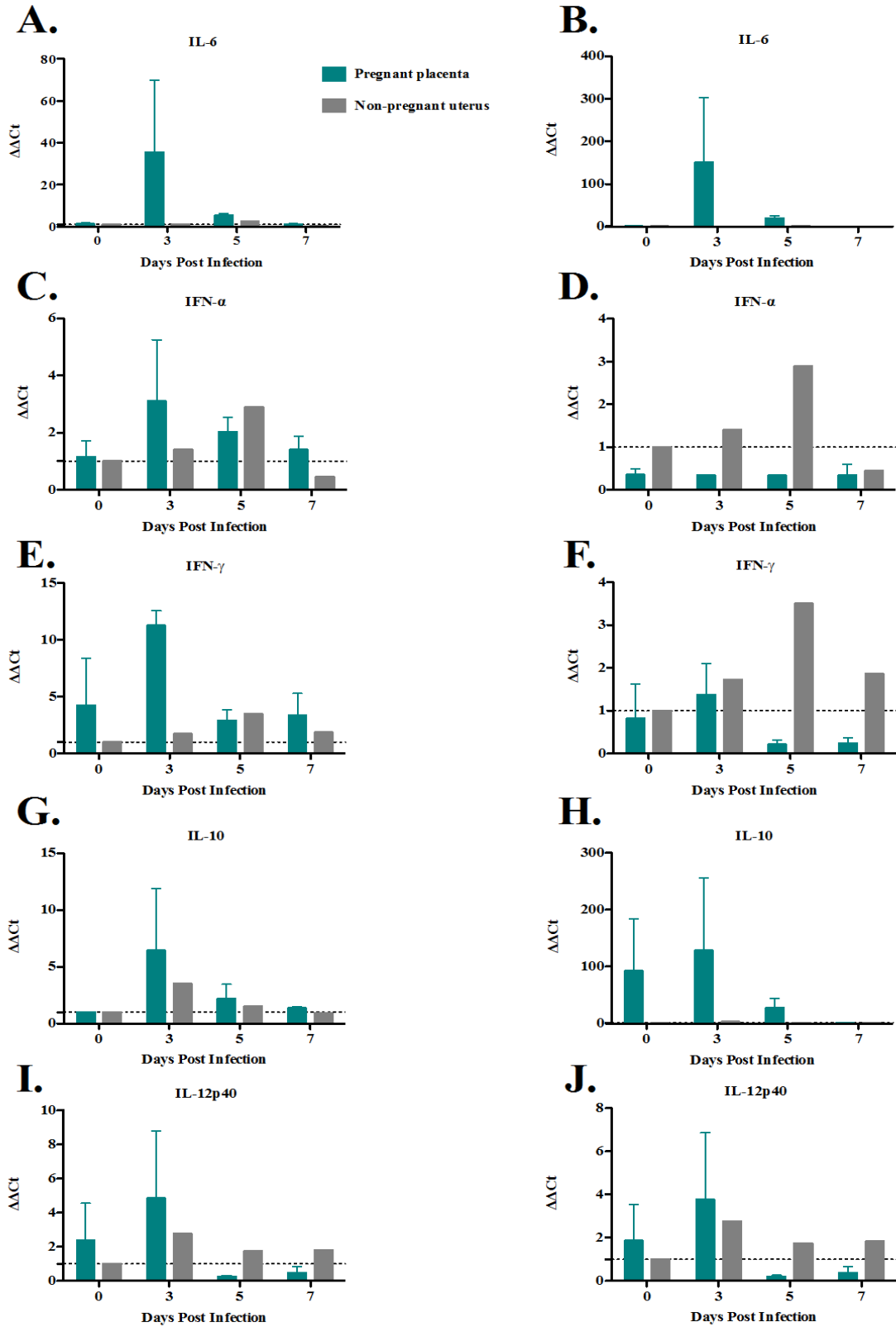**J.** IL-12p40 — ΔΔCt vs Days Post Infection

Figure 10. Cytokine levels in the placental tissue of pregnant and uterine tissue of non-pregnant ferrets infected with A/California/04/09.

Two ferrets from each of the pregnant and non-pregnant groups on day 0, 3, 5, and 7 were sacrificed. Placenta and uterus samples were assessed for cytokine messenger RNA expression (n=2 per time point) using RT-PCR and are represented as the mean fold change (standard deviation) compared to the values of their own reference group (a) and (b) compared to the day 0 non-pregnant ferret group. **(A)** Interleukin 6 (IL-6) mRNA levels in the placenta and uterus homogenates of pregnant and non-pregnant ferrets compared back to their own group day 0 time point. **(B)** IL-6 mRNA levels in the placenta and uterus homogenates of pregnant and non- pregnant ferrets compared back to the non-pregnant day 0 time point. **(C)** Interferon α (IFN-α) mRNA levels in the placenta and uterus homogenates of pregnant and non-pregnant ferrets compared back to their own group day 0 time point. **(D)** IFN-α mRNA levels in the placenta and uterus homogenates of pregnant and non-pregnant ferrets compared back to the non-pregnant day 0 time point. **(E)** Interferon γ (IFN-γ) mRNA levels in the placenta and uterus homogenates of pregnant and non-pregnant ferrets compared back to their own group day 0 time point. **(F)** IFN-γ mRNA levels in the placenta and uterus homogenates of pregnant and non-pregnant ferrets compared back to the non-pregnant day 0 time point. **(G)** Interleukin 10 (IL-10) mRNA levels in the placenta and uterus homogenates of pregnant and non-pregnant ferrets compared back to their own group day 0 time point. **(H)** IL-10 mRNA levels in the placenta and uterus homogenates of pregnant and non-pregnant ferrets compared back to the non-pregnant day 0 time point. **(I)** Interleukin 12p40 (IL-12p40) mRNA levels in the placenta and uterus homogenates of pregnant and non-pregnant ferrets compared back to their own group day 0 time point. **(J)** IL-12p40 mRNA levels in the placenta and uterus homogenates of pregnant and non-pregnant ferrets compared back to the non-pregnant day 0 time point.

4.3.1.4 Fetus

Based on the previous IL-6 and IL-10 data from other tissues and the role of IL-6 in fetal inflammatory response syndrome we focused on these cytokines in the fetus. IL-6 and IL-10 mRNA levels in the fetus of the pregnant ferrets increased over pregnant reference placenta at day 3 and 5 PI and subsequently decreased to base levels by day 7 PI (Figure 11).
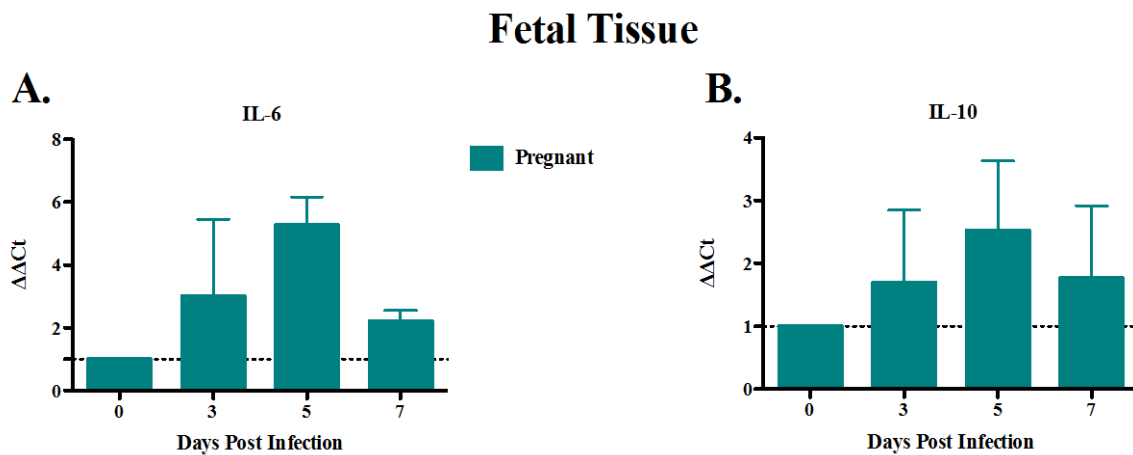
Figure 11. Cytokine levels in the fetal tissue of pregnant ferrets infected with A/California/04/09.

Fetal samples were assessed for cytokine messenger RNA expression (n=2 per time point) using RT-PCR and are represented as the mean fold change (standard deviation) compared to the values of their own reference group at day 0 time point. **(A)** Interleukin 6 (IL-6) mRNA levels in the fetal homogenates of pregnant ferrets. **(B)** IL-10 mRNA levels in the fetal homogenates of pregnant ferrets.

4.3.2 Monitor Development of Antibody Response

Pregnant and non-pregnant ferrets demonstrated a similar evolution of influenza specific antibody titers in sera for the first 7 days post infection (Figure 12). There may be a slight delay in onset of antibody titer in the pregnant group at day 3 and 5 PI however by day 7, both groups had analogous antibody responses.
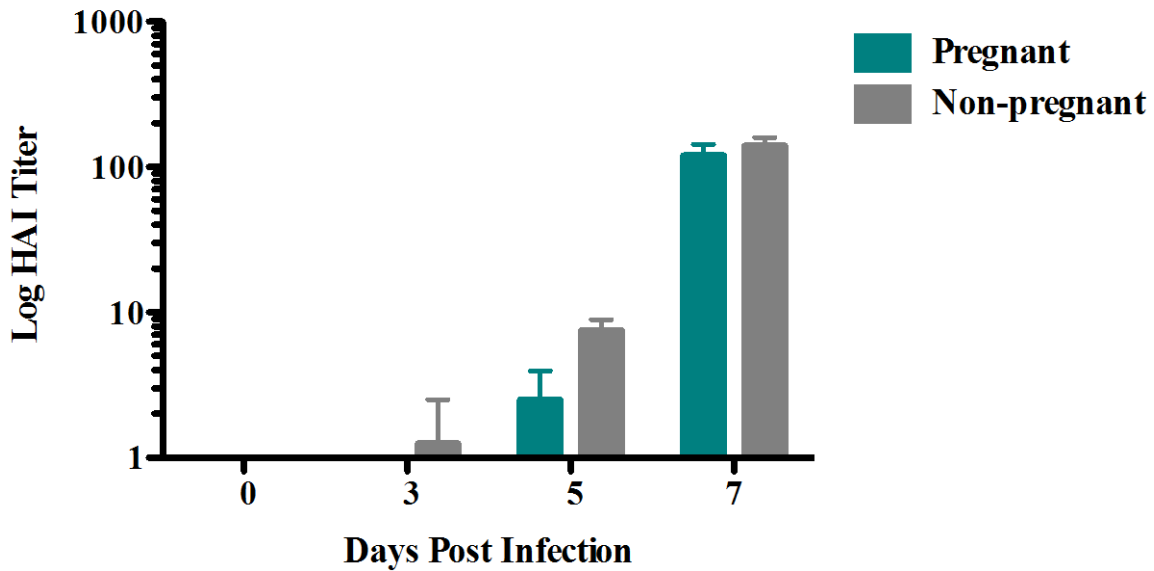
Figure 12. Serum antibody responses to aerosol exposure of pH1N1.

Sera collected from pregnant and non-pregnant ferrets post aerosol exposure to pH1N1 was assayed for the presence of antibodies using a hemagluttination inhibition assay.

4.3.3   Summary of Aim 2

Semi-quantitative RT-PCR revealed differences in basal levels of cytokine mRNA levels as well as differences in the responses of pregnant versus non-pregnant ferrets over the course of infection in the lung, spleen, placenta and fetus. Notably, IL-6 and IL-10 were both found at higher mRNA transcript levels in the lung, placenta and fetus but not in the spleen of the pregnant ferrets compared to the non-pregnant ferrets. Alternatively, IFN-γ displayed similar transcript levels in both the pregnant and non-pregnant ferret groups over the course of infection in the lung, spleen, placenta and uterus. These differences in cytokine response did not lead to a difference in ability between the two cohorts ability to mount an effective humoral immune response.

5.0   DISCUSSION

The pregnant ferret group exhibited more severe clinical disease compared to a non-pregnant ferret control group when challenged with pandemic 2009 H1N1, highlighted by the pregnant ferrets' greater weight loss, lethargy, poor oral intake, and respiratory symptoms compared to the non-pregnant ferret group. The greater weight loss experienced by the pregnant ferrets was particularly problematic, occurring at a time when they should be gaining weight. This may contribute to low fetal birth weight, and possibly premature birth. The observed outcomes in pregnant ferrets compared to the age-matched controls paralleled what was seen in humans and demonstrates the validity of this animal model.

The greater severity of clinical manifestations in the pregnant ferrets was not due to a larger viral burden or differential dissemination differences. Both ferret groups had similar levels of virus present in the lung and brain over the course of infection. Brain dissemination is not common after intranasal challenge of influenza infection in the ferret model, but the use of aerosol challenge has not been thoroughly investigated. Further experimentation is needed to discern the possibility of influenza disseminating to the brain through the central nervous system or more likely, entering through the olfactory bulb.

Vertical transmission of pH1N1 in the pregnant human population was rarely reported during the H1N1 pandemic[17]. Here, viral presence was noted in the placenta and fetus of the pregnant ferrets. Due to the inability to accurately measure replication competent virus, it can

only be concluded that there are viral copies at this site. It is possible that viral presence at the maternal/fetal interface is sufficient to contribute to a difference in immunological response at these sites and lead to greater influenza pathogenicity[29]. Pathology did not reveal any significant differences in the lungs between the pregnant and non-pregnant ferret group. These lung pathology findings contradict a previous study demonstrating that pH1N1 infection in pregnant mice was not due to enhanced viral burden, but associated with lung immunopathology and impaired lung repair[43]. Placental pathology revealed villi apoptosis of the pregnant ferrets at 5 and 7 PI, suggesting possible immune activation or the start of preterm delivery.

Interestingly, IL-6 and IL-10 were up-regulated at the mRNA gene expression level in the pregnant ferret group compared to the non-pregnant ferret group in the lung and at the maternal/fetal interface, but not in the spleen. IL-6 is a Th2 pro-inflammatory cytokine that can be induced by inflammatory stimuli, and IL-10 is a major immune modulatory cytokine mainly thought to suppress Th1 cytokine production. Both IL-6 and IL-10 mainly act via through the Janus (Jaks) and STAT signal transduction pathways and share some common biological activities[44,45]. IL-6 can induce expression of IL-10 to some extent,[46] and work in concert to clear pathogens and regulate cellular immune responses, which are critical to host protection but can result in destructive tissue inflammation.

IL-6 has previously been linked to an increased inflammatory response in humans to seasonal influenza infection including high fever, phagocytic cell recruitment, and blood vessel permeability[47–49]. Increased cytokine production upon pH1N1 infection in humans has been thought to contribute to pathogenesis, and recently it has been demonstrated that high sera cytokine levels of IL-6 and IL-10 were found in patients with severe pH1N1 infection compared to non-influenza like illness infection patients and healthy controls[27,44]. Severely infected pH1N1

patients generally had pulmonary inflammation leading to acute respiratory distress and death. Further IL-6 production has been postulated as a potential biomarker for severe disease caused by pH1N1. The mechanism for IL-6 contributing to disease progression during pH1N1infection was preliminarily investigated using an IL-6 -/- mouse model, but did not result in a clear mechanism[28]. IL-6 -/- mice did not demonstrate significant difference in survival or weight loss compared to wild type, nor were any differences found in viral loads or lung pathology. Similarly, we found higher mRNA levels of IL-6 and IL-10 in the lung, but paradoxically, no significant differences were observed in lung pathology between the two groups. This suggests another mechanism apart from pulmonary inflammation, leading to pulmonary damage.

IL-6 and IL-10 levels were also higher in the placentas of the pregnant ferrets compared to the uterus of the non-pregnant ferrets, and these cytokines were found in the fetus of the pregnant ferrets by day 3 PI and continuing throughout infection. This observation, along with mild pathology observed in the placenta, suggests that pH1N1 infection during late stage pregnancy elicits a pro-inflammatory response at the maternal/fetal interface that could lead to placental damage, abortion, or preterm labor. Previous studies have indicated that TNF-α, IFN-γ, IL-12, and IL-6 production during pregnancy can activate the maternal immune system, and lead to poor pregnancy outcomes[29]. Conceivably, pregnant women infected with pH1N1 could activate a detrimental immune response at the maternal/fetal interface, contributing to increased rates of premature birth and abortive pregnancy.

The dysregulation of cytokine response in the pregnant ferrets as compared to the non-pregnant ferrets did not result in differences in antibody responses. Both groups had comparable antibody titers by day 5 PI.

To conclude, pregnant ferrets demonstrated a greater clinical course of disease compared to the age-matched controls, but this was not due to differences in viral loads, viral dissemination, lung pathology, or antibody responses. Differences in mRNA cytokine levels in the lung and at the maternal/fetal interface suggest that pregnant ferrets have a dysregulated cytokine response, most notably an up-regulation of IL-6 and IL-10. It could be postulated that the difference in cytokine milieu, especially in the initial stages of infection, could lead to a differential response where pregnant ferrets could have a less effective cell-mediated and/or natural killer (NK) cell response, resulting in more severe disease. Historically, IL-6 and IL-10 have been implicated in severe pH1N1 infection, suggesting that IL-6 could increase vascular permeability causing more significant disease in the lungs of the pregnant ferrets[49]. IL-6 could also activate the maternal and fetal immune response leading to poor gestational outcomes.

5.1.1   Hypothesized Model

If the pregnant ferret model accurately mimics pH1N1 infection in pregnant humans, it could be postulated that pregnancy creates a skewed immune response, in which the initial response to pH1N1 virus is first recognized by the innate immune system, leading to an abnormal release of pro-inflammatory cytokines in lung, placenta, and fetal tissue. The production of IL-6 and IL-10 in these tissues may lead to disease progression by an unknown mechanism. IL-6 and IL-10 induction have been well documented in severe pH1N1 infection, leading to acute respiratory distress and possibly death, although the mouse model has not been linked with greater pathology in the lung. Further investigation on the underlying mechanism of disease progression is necessary. Furthermore, IL-6 has been implicated in premature birth and other adverse maternal/fetal outcomes, suggesting that activation of an immune response at the

fetal /maternal interface could contribute to poor outcomes such as those seen during the H1N1 pandemic[29].

We propose an influenza infection model where upon infection with pH1N1 in pregnant women induces a dysregulated cytokine response in lungs and at the maternal/fetal interface, leading to negative outcomes for the mother and fetus (Figure 13). This abnormal immune response does not lead to significantly different viral load or dissemination, or lung pathology changes, but may lead to vascular permeability in the lungs, or a less effective cell-mediated response and preterm or abortive delivery of the fetus.

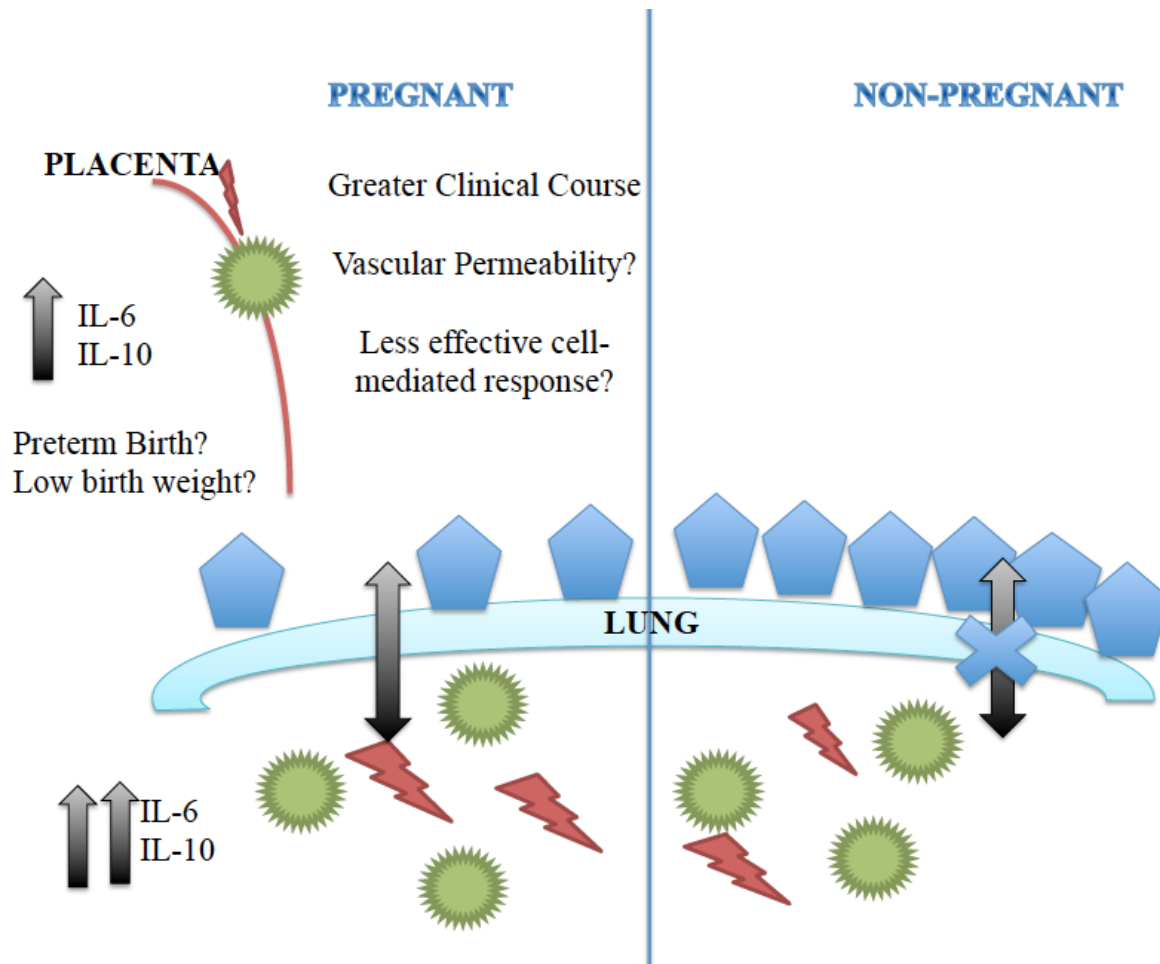**Figure 13**. **Hypothesized Model.**

Both pregnant and non-pregnant ferret groups had comparable viral copies (green) and pathology (red lightening) in the lung (light blue). Pregnant ferrets had low levels of viral copies (green) present in the placenta by day 3 PI and fetus by day 7 PI with mild villi apoptosis present (red lightening). Placenta and fetus also demonstrated higher levels of IL-6 and IL-10.

5.1.2 Future Directions

This study is limited by small sample sizes and a lack of pregnant controls not exposed to influenza to provide a natural history comparison during pregnancy. Future studies that address both these limitations will enhance the quality of the findings and further elucidate the noted clinical differences. Monitoring a natural history of the disease would help determine if pregnant ferrets have greater clinical disease leading to fatal outcomes and/or poor gestational outcomes similar to humans. A larger serial sacrifice study would aid in dissecting the mechanism(s) responsible for increased severity of clinical disease in pregnant ferrets by further investigating immunopathology and immune responses. Lastly, experiments would be aimed at assessing the basic therapeutic questions of when, and what, will best ameliorate the effects of disease, especially during pregnancy.

5.1.3 Public Health Significance

It is essential that non-traditional animal models be established to answer important public health questions. For influenza infection, important non-traditional animal models could assist in answering fundamental questions about why the young, elderly and pregnant women are more severely affected. Pandemic H1N1 reminded the public health community that little is known about the mechanism by which pregnant women are more severely affected and/or more susceptible to certain infectious diseases. By establishing pertinent animal models, questions of why pregnant women are more susceptible or have more severe clinical outcomes and how viral infections affect the fetus and pregnancy outcome could be investigated.

Influenza vaccination coverage among pregnant women has been historically low, generally <10% of the population, and especially insufficient when compared to other groups with increased risk for complications[50]. However, in 2009, with the emergence of pH1N1, coverage rates jumped to 45% in the United States, still highlighting a substantial coverage gap and illustrating the need for therapeutics[50]. Pregnant women represented 6.3% of hospitalizations, 5.9% ICU admissions, and 5.7% of pH1N1 deaths in the United States while only making up approximately 1% of the population[17]. Importantly, an animal model could answer translational questions about the effectiveness of therapeutics and when treatment would be most effective, potentially lowering the amount of lives lost, hospitalization rates, and economic burden.

APPENDIX

EXPERIMENTAL PROCEDURES

A. Materials and equipment

- Pipettes
- MDCK cells (ATCC CCL-34)
  Currently in LN2 storage (KSC – Box 4B Row D 3/6/09 AH)
- MDCK maintenance media

500ml	D-MEM (with 4.5 g/L glucose, 4mM L-glutamine #10-017 CV Mediatech or 11965-092 Gibco)
5ml	Penicillin/Streptomycin (10,000U/ml/10,000 ug/ml)
5ml	HEPES Buffer (1M stock)
5ml	L-glutamine, 200 mM (100X) (if needed)
25ml	Heat Inactivated FBS

- Virus Dilution Media

500ml	D-MEM (with 4.5 g/L glucose, 4mM L-glutamine)
5ml	Penicillin/Streptomycin (10,000 U/ml / 10,000 ug/ml)
12.5ml	Bovine Serum Albumin fraction V, 7.5% solution in PBS
5ml	HEPES Buffer (1M stock)

- Viral Growth Media (Virus Dilution Media + TPCK trypsin)

100ml	Virus Dilution Media
0.1ml	1:1000 2mg/ml TPCK-trypsin (2µg/ml) stock added at time of use Stock: dissolve 20mg TPCK trypsin (type XIII from bovine Pancreas) in 10ml of dH20, sterile filter through 0.2 µm membrane, store at -20°C.

- 2x DMEM media

  DMEM powder (Gibco 31600-034, w/ L-glutamine, sodium pyruvate, pyridoxine HCl)

Hi-Glucose Glucose (4.5g/L total, if low glucose (1g/L) is used, add 3.5g/L extra)
NaHCO$_3$ (3.7g/L)
Prepare as double concentrated liquid, ½ volume of water for dry ingredients
pH to 7.4
Sterile filter and store at 4°C

- 2% Agarose solution

  Autoclave sterile 2% agarose (Invitrogen, Ultra-pure, 15510-027) in MQH$_2$0. Store at room temperature.
- Freezing media

    50% FBS
    40% DMEM
    10% cell culture grade DMSO
    Sterile filter and store aliquots at -20°C
- Phosphate buffered saline pH 7.2 (PBS)
- Cell culture grade trypsin-EDTA solution (0.25%)
- Influenza Viruses
- A/California/04/09 (H1N1) – obtained from St. Jude Children's Research Hospital. RBL stock 6/18/09, AH 3x10^6 TCID50/ml p1 in MDCK
- 5% Turkey RBC solution (Alsever's), Lampire Biolabs # 7249409
- 0.4 % Trypan Blue solution
- Hemacytometer
- Humidified incubator, 37°C, 5% CO$_2$
- 96 well tissue culture flat bottom plates
- 96 well tissue culture vee-bottom plates
- TC-6 well plates
- T-25,75, 125 cm^2 vented flasks
- Multichannel pipettemen 50-300 µl, 5-50 µl
- Class II Biological safety cabinet
- Inverted phase contrast microscope

B.   MDCK cells propagation
   i. Thaw cells/initiate culture
      1. Quick thaw cells from LN2 in 37 °C water bath.
      2. Resuspend in 10ml maintenance media
      3. Centrifuge 400g for 5 minutes
      4. Dump supernatant
      5. Resuspend in 8ml maintenance media
      6. Add cell suspension to T25 flask with vented cap
      7. Incubate for 24-36 hrs. at 37°C/5% CO2
   ii. Maintenance/splitting
      1. Cells should be split 1:10 every 3-4 days
      2. Dump growth media

3. Wash cells twice with PBS (warmed to 37°C)
4. Add 0.25% trypsin/EDTA (warmed to 37°C)
   2ml for T75, 4 ml for T150
5. Place flask in incubator until cells round up and dislodge (4-8min) when the flask is tapped from the side
6. Resuspend cells in 5:1 volume of maintenance media:trypsin washing residual cells from flask surface and triturating gently
7. Dispense 1:10 volume to a fresh flask
8. Incubate at 37°C/5% CO2
   Note: MDCK cells should not be used more the passage twenty for productive influenza replication

iii. Freezing
1. Collect MDCK cells at 80-90% confluency (log phase growth) using steps ii.2-6
2. Count total viable cells using trypan blue assay
3. Resuspend cells at ~10^7 cells per ml in freezing media
4. Aliquot 1ml into cryovials
5. Place aliquots into freezing vessel indicated for 1°C/hour rate
6. Place vessel into -80°C freezer
7. After 48-72 hours transfer vials to LN2 for long term storage

C.   Preparation of influenza virus stocks in MDCK cells
i. Split MDCK cells as per maintenance protocol, culturing into multiple T-150 flasks (use MDCK cells of passage 5-15 only)
ii. At ~90% confluency within 24 hours of culture
iii. Dump supernatant, wash cells 3x with virus growth media
iv. Dilute inoculating virus to 0.1-10 moi (depending on strain of virus) in 2ml of virus growth media for each flask
   1.   Assume ~10^7 MDCK cells at 90% confluency in T-150
v. Apply virus to MDCK monolayer in flask
vi. Incubate for 45 minutes at 37°C/5% CO_2, rocking the flask every 10minutes to distribute the inoculum
vii. Add 60ml virus growth media to the flasks
viii. Incubate at 37°C/5% CO_2 until 3-4 CPE is observe (dependent on virus strain, non CPE viruses may be harvested ~48-72 hours)
ix. Add 2.5ml 7.5% BSA to each flask (0.5% total BSA concentration)
x. Optional step 1: freeze flask at -80C prior to harvesting supernatant
   1.   Quick thaw on 37C water bath, sonicate sample in flask and then proceed to centrifuging sample. Freeze/thaw and sonication may help recover cell associated virus, but could reduce infectious free virus.
xi. Collect supernatant in 50 ml conical tubes and centrifuge 600g x 10 min at 4°C to pellet debris
xii. Optional step 2: filter supernatant through 0.2 µM filter to obtain virus only fluid
xiii. Dispense supernatant into 1ml cryovials and freeze aliquots at -80°C

xiv. Streak 1ml and 0.5ml samples onto BAP for sterility test
1. Incubate plate for up to 96 hours at 37°C
2. Anaerobe culture may also be performed if suspect or required for lot verification
xv. Verify titer of frozen stock with TCID50 or HA assays

D. Hemagglutination (HA) assay

- Important note to HA assay: HA subtype and strain (e.g. H1,H3,H5) have differential binding affinities to RBCs dependent on the species from which the RBCs where obtained. This is due to the sialic acid residue expression on the RBCs. To date we have used turkey RBCs for A/CA/04/09 H1N1. Other strains would need to be validated for species of RBC to obtain accurate HA measurements. Additionally, u-bottom plates may be preferred to vee-bottom depending on species of RBCs used.
  i. Prepare RBCs
      1. Spin 1ml of RBCs at 650RPM, 5min in 15ml tube
      2. Dump supernatant and resuspend in 10ml PBS for 0.5% RBC working solution
  ii. Dilute virus samples
      1. Add 100 µl of virus samples to first column of a v-bottom 96 well plate
      2. Add 50 µl of room temperature PBS to the remaining wells, ensuring that no virus controls have been included
      3. Serial dilute virus 1:2 (50 µl) across the plate with a multichannel pipettman disposing of tips between wells
  iii. Add 50 µl of 0.5% RBC solution to every well
  iv. Agitate plate for 20 seconds to mix samples
  v. Incubate 1 hr at room temperate
  vi. Observe agglutination reaction
      1. Button = no agglutination
      2. Hazy matrix = agglutination
  vii. Record endpoint HA titer (last dilution to demonstrate agglutination)

E. TCDI50 assay
  i. Prepare MDCK cells from a confluent T-75cm$_2$ flask.
      1. Remove culture media.
      2. Wash cell monolayer with 10ml PBS.
      3. Add 2.0ml 0.25% trypsin-EDTA to monolayer and incubate for ~5 minutes.
      4. Collect cells in 10 ml of MDCK maintenance media.
      5. Enumerate cell concentration using standard trypan blue staining visualized with a hemacytometer.
      6. Dilute cells to 3.0×10^5 c/ml in maintenance media.
      7. Dispense 100 uL (3.0×10^4 cells) into each well of 96 well flat bottom plates, 2 samples may be analyzed per plate.

8. Incubate at 37°C, 5% CO_2 until <u>confluent</u> monolayer is obtained (~24-30 hours).
9. Remove media from MDCK cells using aspiration.
10. Wash each well with 200 µl of PBS and remove by aspiration.
11. Add 150 µl of viral growth media to each well containing cells, set plates aside.

ii. Set up virus titrations
1. Add 180 µl of viral growth media to rows B-H of 96-well sterile v-bottom plates using multichannel pipetteman.
2. Add 200 µl of virus sample to each of 5 wells for sample 1 (columns 1-5), sample 2 (columns 6-10) and 200 µl of assay buffer only to column 11 as non-infection control.
3. Using multichannel pipette transfer 20 µl from row A to row B, discard tips.
4. Mix 20 times using swirling tip action and transfer again 20 µl from row B to row C, discard tips.
5. Repeat dilution down the plate.
6. Using multichannel pipette transfer 100 µl of each virus dilution to MDCK cells in 96 well flat bottom plates. Start at lowest concentration (row H) on v-bottom plate and work up using same tips.
7. Incubate plates at 37°C, 5% CO_2.
8. Observe CPE daily and record using attached template.

CPE 0 = no cytopathic effects observed, same as controls
CPE 1= monolayer intact, rounded up cells on top of monolayer with few dead cells
CPE 2= many dead cells, but monolayer intact
CPE 3= most cells destroyed, but some remnants of monolayer observed
CPE 4= monolayer completely destroyed
9. Calculate the TCID50 using the method described by Reed and Meunch[38]

F.   Hemagglutination assay for detection of virus in TCID50 assay
i. See HA assay above (B)
ii. Prepare RBCs as given above
iii. Dispense 50 µl to each well of a 96-well v-bottom plate
iv. Transfer 50 µl of supernatant from TCID50 plate to v-bottom plate so that all wells are corresponding (i.e. A1 = A1…H12=H12)
v. Read reaction after 1 hr incubation at room temperature
vi. Record + or – HA reaction
vii. Calculate TCID50 using Reed Meunch method where + HA is equivalent to + CPE and – HA is equivalent to zero CPE.

G.   Hemagglutination Inhibition assay for detection of influenza specific antibodies

55

    i.   Prepare RBCs
1. Spin 1 mL of RBCs (turkey RBCs of pH1N1) at 650 RPM for 5 minutes
2. Dump supernatant and resuspend in 10mL PBS for a 1% working concentration
    ii. Prepare Ferret Sera
1. Place all sera samples into water bath heated to 56 C for 30 min to heat inactivate
2. Absorb the sera by adding 0.5% TRBC suspension to each microcentrifuge tube making a 1:5 dilution of the original sample (i.e. 50uL sera: 200uL TRBC)
3. Incubate for 30 minutes at RT, mixing the tubes by inverting the tube at 10 min intervals
4. Pellet the TRBC in the tubes by microcentrifuge for 5 seconds at 14,000 RPM
5. Transfer the sera into new microcentrifuge tubes, being careful not to disturb the pellet
    iii. Perform HAI Assay
1. Add 50 uL PBS to all wells in rows B through G of a 96 well vee bottom plate and 100uL to all wells in row H (Control wells)
2. Add 100uL of each serum sample to duplicate, adjacent wells in row A as well as 100uL of each viral antigen control on each plate.
3. Serial Dilute 1:2 across plate starting with row A and ending in row G
4. After mixing the contents of row G, remove and discard 50 uL from row G
5. Dilute H1N1 virus stock to 4 HAU (1:4 dilution)
6. Starting at row G and working up to row A, add 50uL of the virus stock to each well
7. Incubate the plate at RT for 30mins
8. Add 50uL of the 1% TRBC suspension in PBS to all wells starting at row H and working up to row A.
9. Incubate plate for 30-45min at room temperature
10. Read plates for agglutination
11. Record endpoint HA titer (last dilution with a visible button)

H.   **Tissue Homogenization: For preparation of RNA extraction for Viral qPCR**

1. Homogenize Samples in 1 mL of Virus Dilution Media (1-2 g tissue into 2mL VDM)
2. Take 100uL diluted to standard amount of homogenate (100mg) and add to 900 uL TRI Reagent (Sigma catalog #T9424). Allow to sit and room temperature. (Save homogenate for other assays label (15mL conical) as Ferret #, Tissue, Date)

3. Transfer TRI/homogenate to different tube. Label Ferret #, Tissue, Date, TRI.
4. Store at -70C for up to a month

I. **RNA Isolation for Viral qPCR using MagMAX-96 Total RNA Isolation Kit (Invitrogen catalog # AM1830)**

i. RNA Isolation:

1. Transfer homogenized sample to a 1.5 mL microcentrifuge tube. Add 0.1 volumes of BCP (e.g., add 100 µL BCP to 1 mL of homogenate), and cap the tube securely.

2. Vortex at moderate speed for 5–10 seconds. Store the mixture at room temperature for 5min. Centrifuge at 12,000 x g for 10 min at 4°C to separate the sample mixture into three phases: phenol-BCP on the bottom (red), interphase in the center, and aqueous phase on the top (colorless). RNA is in the aqueous phase, while DNA and proteins are in the interphase and organic phase (phenol-BCP).

3. Transfer 100 µL of the aqueous phase to a well of the 96-well Processing Plate and continue the procedure.

ii. RNA Purification Using RNA Binding Beads

1. Add 50 µL of 100% isopropanol and shake for 1 min on an orbital shaker

2. Add 10 µL of RNA Binding Beads (vortex before adding) and shake for 3 min on an orbital shaker

3. Magnetically capture the RNA Binding Beads and discard the supernatant

4. Move the Processing Plate to a magnetic stand to capture the RNA Binding Beads.
Leave the plate on the magnetic stand until the mixture becomes transparent, indicating that capture is complete. The capture time depends on the magnetic stand used. Using the Ambion 96-Well Magnetic-Ring Stand, the capture time is ~1–2 min. Carefully aspirate and discard the supernatant without disturbing the beads, and remove the Processing Plate from the magnetic stand. To obtain pure RNA, it is important to completely remove the supernatant at this step.

iii. Separation of Aqueous and Organic Phases Spin Procedure

5. Wash twice with 150 µL Wash Solution 1min on an orbital shaker each time.

a. Capture the RNA Binding Beads on a magnetic stand as in the previous step.

b. Carefully aspirate and discard the supernatant without disturbing the beads, and remove the Processing Plate from the magnetic stand.

> c. Repeat steps a–b to wash with a second 150 μL of Wash Solution.

6. Move the Processing Plate to the shaker and shake vigorously for 2 min.

7. Dry the beads by shaking for 2 min

8. Elute the RNA in 50 μL of Elution Buffer shake vigorously for 3 min
> a. Capture the RNA Binding Beads on a magnetic stand. The purified RNA will be in the supernatant.
>
> b. Transfer the supernatant, which contains the RNA, to a nuclease-free container appropriate for your application.

J.   Quantitative reverse transcriptase real time PCR (qrRT-PCR) for Pandemic H1N1 Matrix and Nucleoprotein from Tissue Samples [39]

> i.   Invitrogen SuperScript ™III Platinum ® One-Step Quantitative Kit (cat# 11732-020or 11745-100).
> ii. MicroAmp Optical Plates (ABI N801-0560)
> iii. Optical Adhesive covers (ABI #4311975)
> iv. 7900 HT Thermo cycler (ABI)
> v.   Nuclease-free plastics
> vi. DEPC treated H20

Table 3. Matrix and Nucleoprotein Primer and Probes

Set up PCR reaction:

Primers and Probes	Sequence (5'>3')	Working Concentration
InfA Forward	GAC CRA TCC TGT CAC CTC TGA C	40 μM
InfA Reverse	AGG GCA TTY TGG ACA AAK CGT CTA	40 μM
InfA Probe	TGC AGT CCT CGC TCA CTG GGC ACG	10 μM
SW InfA Forward	GCA CGG TCA GCA CTT ATY CTR AG	40 μM
SW InfA Reverse	GTG RGC TGG GTT TTC ATT TGG TC	40 μM
SW InfA Probe	CYA CTG CAA GCC CA"T" ACA CAC AAG CAG GCA	10 μM

Taqman probes are labeled at the 5'-end with the reporter molecule 6-carboxyfluorescein FAM) and quenched internally at a modified "T" residue with BHQ1, with a modified 3'-end to prevent probe extension by Taq polymerase (Biosearch Technologies, Inc.,.Novato, CA).

1.   Reaction assay mixtures are made as a cocktail and dispensed into the 96-well reaction plate. Water and extracted nucleic acid or positive template controls are then added to the appropriate test reactions and controls.
2.   Label one 1.5 ml microcentrifuge tube for each primer/probe set.
3.   Determine the number of reactions (N) to set up per assay. It is necessary to make excess

reaction cocktail to allow for the NTC, PTC, HSC reactions and pipetting error. See below:

4. If number of samples (n) including controls = 1 to 14, then N = n + 1
5. If number of samples (n) including controls > 15, then N = n + 2
6. Master Mix: calculate the amount of each reagent to be added for each primer/probe set reaction master mix. The calculations are as follows:

Table 4. PCR Reagents for Viral qRT-PCR

Reagent	Volume of Reagent Added per Reaction
Nuclease-free Water	N x 5.5 µl
Forward Primer	N x 0.5 µl
Reverse Primer	N x 0.5 µl
Probe	N x 0.5 µl
SuperScript™ III RT/Platinum® Taq Mix	N x 0.5 µl
2X PCR Master Mix	N x 12.5 µl
Total Volume	N x 20.0 µl

After addition of the water, mix reaction mixtures by pipetting up and down. Do not vortex.

7. Centrifuge for 5 sec to collect contents at bottom of the tube, and then place the tube in cold rack.
8. Set up reaction strip tubes or plates in 96-well cooler rack.
9. Dispense 20uL of each master mix into each well as needed.
10. Before moving the plate to the nucleic acid handling area, set up the NTC reactions for column 1 in the assay set-up area. Add 5 uL of nuclease free water as the negative control wells.
11.Cover the reaction plate and move the reaction plate to the nucleic acid handling area.
12.Vortex the tubes containing the samples for 5 sec.. Centrifuge tubes for 5 sec.
13.Set up the extracted nucleic acid samples in the cold rack.
14.Pipette 5 uL of samples into the wells labeled for that sample. Change tips after each addition.
15.Cap the column to which the sample has been added. This will help to prevent sample cross contamination and enable you to keep track of where you are on the plate.
16.Repeat steps 13-15 for the remaining samples.
17. Note: for quantitative analysis, Viral standards must run on each plate using 10^6 – 10^0 copy/well in 1:10 dilutions in duplicate
18. Perform amplification/analysis
    a. Open Template on 7900HT ABI
    b. Designate standards from SDS software menu
    c. Designate unknowns
    d. Ensure parameters are correct below.

Table 5. Influenza Detection Program

The reaction voume is 25 µL. Program the thermocycler as follows:

Reverse Transcription	50°C for 30 min
Taq inhibitor activation	95°C for 2 min
PCR amplification (40 cycles)	95°C for 15 sec 55°C for 30 sec*

Fluorescence data (FAM) should be collected during the 55°C incubation step.

- Dissociation Curve
  55-95°C, 100%-20%
  ROX reference
  FAM channel
  25ul sample
  e. Load plate
  f. Start machine
  g. At completion of run, save data as SDS file
  h. Analyze data (compare to standard curve of TCID50).

K.　　**RNA Isolation for mRNA semi-quantitative RT-PCR of cytokines using RNeasy Mini Kit from Qiagen (cat. # 774104) and On-column Dnase Digestion (cat.# 79254)**

1. Tissues: Do not use more than 30 mg tissue. Disrupt the tissue and homogenize the lysate in the appropriate volume of Buffer RLT. Centrifuge the lysate for 3 min at maximum speed. Carefully remove the supernatant by pipetting, and use it in step 2.

2. Add 1 volume of 70% ethanol to the lysate, and mix well by pipetting. Do not centrifuge. Proceed immediately to step 3.

3. Transfer up to 700 uL of the sample, including any precipitate, to an RNeasy Mini spin column placed in a 2 ml collection tube (supplied). Close the lid, and centrifuge for 15 s at > 8000 x g. Discard the flow through.

4. Add 350 uL Buffer RW1 to RNeasy column, close lid, centrifuge for 15 s at > 8000 x . Discard flow-through.

5. Add 10 uL DNase 1 stock solution to 70uL Buffer RDD. Mix by gently inverting the tube. Centrifuge briefly.

6. Add DNase I incubation mix (80uL) directly to RNeasy column membrane, and place on the bench top (20-30C) for 15min.

7. Add 350 uL Buffer RW1 to RNeasy column, close lid, centrifuge for 15 s at >8,000 x g. Discard flow-through. Continue with step 5 RNeasy Mini Kit.

8. Add 500uL Buffer RPE to the RNeasy spin column. Close the lid, and centrifuge for 15 s at >8,000 x g. Discard flow-through.

9. Add 500uL Buffer RPE to the RNeasy spin column. Close the lid, and centrifuge for 15 s at >8,000 x g. Discard flow-through.
10. Place the RNeasy spin column in a new 2 mL collection tube (supplied). Centrifuge at full speed for 1 min to dry the membrane.
11. Place the RNeasy spin column in a new 1.5 mL collection tube (supplied). Add 30-50uL RNase-free water directly to the spin column membrane. Close the lid, and centrifuge for 1 min at >8,000 x g to elute the RNA.
12. If the expected RNA yield is > 30 ug, repeat step 8 using another 30-50uL of RNase-free water, or using the elute from step 7 (if high RNA concentration is required), Reuse the collection tube from step 8.
13. Nanodrop for RNA purity and concentration

L.   cDNA Synethesis for semi-quantitative RT-PCR: Maxima First Strand cDNA synthesis kit for RT-PCR Thermo Scientific (cat # K1642)
The first strand cDNA synthesis reaction can be performed as an individual reaction or as a series of parallel reactions with different RNA templates. Therefore, the reaction mixture can be prepared by combining reagents individually or a master mix containing all of the components for the RT reaction except template RNA.
After thawing, mix and briefly centrifuge the components of the kit. Store on ice.
1. Add into a sterile, RNase-free tube on ice in the indicated order:

5X Reaction Mix	4 µL
Maxima Enzyme Mix	2 µL
Template RNA	1 µg
Water, nuclease-free to	20 µL
Total volume	20 µL

2. Mix gently and centrifuge.
3. Incubate for 10 min at 25°C followed by 15 min at 50°C.
Note. For RNA template amounts greater than 1 µg, prolong the reaction time to 30 min. For RNA templates that are GC-rich or have a large amount of secondary structure, the reaction temperature can be increased to 65°C.
4. Terminate the reaction by heating at 85°C for 5 min.
The product of the first strand cDNA synthesis can be used directly in qPCR or stored at -20°C for up to one week. For longer storage, -70°C is recommended. Avoid freeze/thaw cycles of cDNA.

Needed Controls:
Negative control reactions should be used to verify the results of the first strand cDNA synthesis.
☐ Reverse transcriptase minus (RT-) negative control is important in RT-qPCR reactions to assess for genomic DNA contamination of the RNA sample. The control RT- reaction should contain every reagent for the reverse transcription reaction except for the Maxima Enzyme Mix.
☐ No template control (NTC) is important to assess for reagent contamination. The NTC reaction should contain all reagents for the reverse transcription reaction except for the RNA template.

M.   Maxima SYBR Green/ROX qPCR Master Mix (2x) Thermo Scientific (cat # K0221)[40,41]

Table 6. Cytokine Ferret Primers

Primers	Sequence (5'>3')
IFNα Foward	ATGCTCCTGCGACAAATGAGGAGA
IFNα Reverse	TTCTGCAGCTGCTTGCTGTCAAAC
IFNγ Foward	CCATCAAGGAAGACATGCTTGTCAGG
IFNγ Reverse	CTGGACCTGCAGATCATTCACAGGAA
TNFα Forward	TGGAGCTGACAGACAACCAGCTAA
TNFα Reverse	TGATGGTGTGGGTAAGGAGCACAT
IL6 Forward	CAAATGTGAAGACAGCAAGGAGGCA
IL6 Reverse	TCTGAAACTCCTGAAGACCGGTAGTG
IL10 Forward	TCCTTGCTGGAGGACTTTAAGGGT
IL10 Reverse	TCCACCGCCTTGCTCTTATTCTCA
IL12p40 Forward	ATCGAGGTTGTGGTGGGTGCTATT
IL12p40 Reverse	TAGGTTCATGGGTGGGTCTGGTTT
GAPDH Forward	AACATCATCCCTGCTTCCACTGGT
GAPDH Reverse	TGTTGAAGTCGCAGGAGACAACCT

Set up PCR

1.   Gently vortex and briefly centrifuge all solutions after thawing.
2.   Prepare a reaction master mix by adding the following components (except template DNA) for each 10 µl reaction to a tube at room temperature: Maxima SYBR Green/ROX qPCR Master Mix (2X)* and for each primer set using the reagents listed in Table 7 below.

Table 7. PCR Reagents

Reagent	Volume of Reagent Added per Reaction
Maxima SYBR Green 2x	N x 5.0 µl
Forward Primer	N x 0.5 µl (.5 µM)
Reverse Primer	N x 0.5 µl(.5 µM)
Template cDNA	1.0 µl
Nuclease Free Water	N x 3.0 µl
Total Volume	*N x 10.0 µl*

3. Mix the master mix thoroughly and dispense appropriate volumes into PCR tubes or plates.
4. Add template DNA (≤500 ng/reaction) to the individual PCR tubes or wells containing the master mix. Note. For two-step RT-qPCR, the volume of the cDNA added from the RT reaction should not exceed 10% of the final PCR volume.
5. Gently mix the reactions without creating bubbles (do not vortex). Centrifuge briefly if needed. Bubbles will interfere with fluorescence detection.

6. Program the thermal cycler according to the recommendations below, place the samples in the cycler as seen below and start the program.

Needed controls :

☐No template control (NTC) is important to assess for reagent contamination or primer dimers. The NTC reaction contains all components except template DNA.

☐ Reverse Transcriptase Minus (RT-) control is important in all RT-qPCR experiments to assess for RNA sample contamination with genomic DNA. The control RT- reaction contains all components for RT-qPCR except the RT enzyme.

Table 8. Gene Expression Program

The reaction volume is 10 µL. Program the thermocycler as follows:

Denaturation	95°C for 15 min
PCR amplification (40 cycles)	95°C for 5s 60°C for 15 sec 72°C for 25 sec*

* SYBR Green data should be collected during the 72°C incubation step.

7. Expression levels were normalized to Glyceraldehyde-3-Phosphate Dehydrogenase (GAPDH) and are reported as fold change compared with day 0 animals based on the ΔΔCt method. To obtain the ΔCt, GAPDH Ct value was subtracted from the gene of interest at each time point. The fold change is calculated by subtracting the day 0 ΔCt values from the subsequent days ΔCt values. To obtain these values as absolute values, the formula: fold change $= 2^{-\Delta\Delta CT}$ is used[42].

BIBLIOGRAPHY

1. Medina, R. A. & García-Sastre, A. Influenza A viruses: new research developments. *Nat. Rev. Microbiol.* **9**, 590–603 (2011).
2. Taubenberger, J. K. & Kash, J. C. Influenza virus evolution, host adaptation, and pandemic formation. *Cell Host Microbe* **7**, 440–451 (2010).
3. Fields, B. N. & Knipe, D. M. *Fields' virology 5.* (Raven Press: New York, NY, 2007).
4. Air, G. M. Sequence relationships among the hemagglutinin genes of 12 subtypes of influenza A virus. *Proc. Natl. Acad. Sci. U.S.A.* **78**, 7639–7643 (1981).
5. Dawood, F. S. *et al.* Emergence of a novel swine-origin influenza A (H1N1) virus in humans. *N. Engl. J. Med.* **360**, 2605–2615 (2009).
6. Neumann, G., Noda, T. & Kawaoka, Y. Emergence and pandemic potential of swine-origin H1N1 influenza virus. *Nature* **459**, 931–939 (2009).
7. Fraser, C. *et al.* Pandemic Potential of a Strain of Influenza A (H1N1): Early Findings. *Science* **324**, 1557–1561 (2009).
8. Update: infections with a swine-origin influenza A (H1N1) virus--United States and other countries, April 28, 2009. *MMWR Morb. Mortal. Wkly. Rep.* **58**, 431–433 (2009).
9. Cheng, V. C. C., To, K. K. W., Tse, H., Hung, I. F. N. & Yuen, K.-Y. Two years after pandemic influenza A/2009/H1N1: what have we learned? *Clin. Microbiol. Rev.* **25**, 223–263 (2012).
10. Girard, M. P., Tam, J. S., Assossou, O. M. & Kieny, M. P. The 2009 A (H1N1) influenza virus pandemic: A review. *Vaccine* **28**, 4895–4902 (2010).
11. Kasowski, E. J., Garten, R. J. & Bridges, C. B. Influenza pandemic epidemiologic and virologic diversity: reminding ourselves of the possibilities. *Clin. Infect. Dis.* **52 Suppl 1**, S44–49 (2011).
12. Dawood, F. S. *et al.* Estimated global mortality associated with the first 12 months of 2009 pandemic influenza A H1N1 virus circulation: a modelling study. *The Lancet Infectious Diseases* **12**, 687–695 (2012).
13. Reed, C. *et al.* Estimates of the Prevalence of Pandemic (H1N1) 2009, United States, April–July 2009. *Emerging Infectious Diseases* **15**, 2004–2007 (2009).
14. To, K. K. W. *et al.* Concurrent comparison of epidemiology, clinical presentation and outcome between adult patients suffering from the pandemic influenza A (H1N1) 2009 virus and the seasonal influenza A virus infection. *Postgraduate Medical Journal* **86**, 515–521 (2010).
15. Zimmer, S. M. *et al.* Seroprevalence Following the Second Wave of Pandemic 2009 H1N1 Influenza in Pittsburgh, PA, USA. *PLoS ONE* **5**, e11601 (2010).
16. Jamieson, D. J. *et al.* H1N1 2009 influenza virus infection during pregnancy in the USA. *Lancet* **374**, 451–458 (2009).

17. Mosby, L. G., Rasmussen, S. A. & Jamieson, D. J. 2009 pandemic influenza A (H1N1) in pregnancy: a systematic review of the literature. *American Journal of Obstetrics and Gynecology* **205**, 10–18 (2011).

18. Fiore, A. E. *et al.* Prevention and control of influenza with vaccines: recommendations of the Advisory Committee on Immunization Practices (ACIP), 2010. *MMWR Recomm Rep* **59**, 1–62 (2010).

19. Ferguson, N. M. *et al.* Strategies for mitigating an influenza pandemic. *Nature* **442**, 448–452 (2006).

20. Interim results: influenza A (H1N1) 2009 monovalent vaccination coverage --- United States, October-December 2009. *MMWR Morb. Mortal. Wkly. Rep.* **59**, 44–48 (2010).

21. Cox, R. J., Brokstad, K. A. & Ogra, P. Influenza Virus: Immunity and Vaccination Strategies. Comparison of the Immune Response to Inactivated and Live, Attenuated Influenza Vaccines. *Scandinavian Journal of Immunology* **59**, 1–15 (2004).

22. Chen, G. L., Lau, Y.-F., Lamirande, E. W., McCall, A. W. & Subbarao, K. Seasonal influenza infection and live vaccine prime for a response to the 2009 pandemic H1N1 vaccine. *Proceedings of the National Academy of Sciences* **108**, 1140–1145 (2011).

23. Fiore, A. E. *et al.* Antiviral agents for the treatment and chemoprophylaxis of influenza --- recommendations of the Advisory Committee on Immunization Practices (ACIP). *MMWR Recomm Rep* **60**, 1–24 (2011).

24. Bautista, E. *et al.* Clinical aspects of pandemic 2009 influenza A (H1N1) virus infection. *N. Engl. J. Med.* **362**, 1708–1719 (2010).

25. Childs, R. A. *et al.* Receptor-binding specificity of pandemic influenza A (H1N1) 2009 virus determined by carbohydrate microarray. *Nat. Biotechnol.* **27**, 797–799 (2009).

26. Brydon, E. W. A., Morris, S. J. & Sweet, C. Role of apoptosis and cytokines in influenza virus morbidity. *FEMS Microbiology Reviews* **29**, 837–850 (2005).

27. Lee, N. *et al.* Cytokine Response Patterns in Severe Pandemic 2009 H1N1 and Seasonal Influenza among Hospitalized Adults. *PLoS ONE* **6**, e26050 (2011).

28. Paquette, S. G. *et al.* Interleukin-6 Is a Potential Biomarker for Severe Pandemic H1N1 Influenza A Infection. *PLoS ONE* **7**, e38214 (2012).

29. Mor, G. & Cardenas, I. The immune system in pregnancy: a unique complexity. *Am. J. Reprod. Immunol.* **63**, 425–433 (2010).

30. Yip, L., McCluskey, J. & Sinclair, R. Immunological aspects of pregnancy. *Clinics in Dermatology* **24**, 84–87 (2006).

31. Denney, J. M. *et al.* Longitudinal modulation of immune system cytokine profile during pregnancy. *Cytokine* **53**, 170–177 (2011).

32. Daher, S. *et al.* Cytokines in recurrent pregnancy loss. *Journal of Reproductive Immunology* **62**, 151–157 (2004).

33. Jamieson, D. J., Theiler, R. N. & Rasmussen, S. A. Emerging infections and pregnancy. *Emerging Infect. Dis.* **12**, 1638–1643 (2006).

34. Erlebacher, A. Immunology of the Maternal-Fetal Interface. *Annual Review of Immunology* **31**, 130108114109008 (2012).

35. Belser, J. A., Katz, J. M. & Tumpey, T. M. The ferret as a model organism to study influenza A virus infection. *Disease Models & Mechanisms* **4**, 575 –579 (2011).

36. Gustin, K. M. *et al.* Influenza virus aerosol exposure and analytical system for ferrets. *Proceedings of the National Academy of Sciences* **108**, 8432–8437 (2011).

37. WHO | Swine influenza. at <http://www.who.int/mediacentre/news/statements/2009/h1n1_20090425/en/index.html>

38. Reed, L. J. & Muench, H. A Simple Method of Estimating Fifty Per Cent Endpoints. *American Journal of Epidemiology* **27**, 493 –497 (1938).

39. Shu, B. *et al.* Design and Performance of the CDC Real-Time Reverse Transcriptase PCR Swine Flu Panel for Detection of 2009 A (H1N1) Pandemic Influenza Virus. *Journal of Clinical Microbiology* **49**, 2614 –2619 (2011).

40. Svitek, N. & von Messling, V. Early cytokine mRNA expression profiles predict Morbillivirus disease outcome in ferrets. *Virology* **362**, 404–410 (2007).

41. Maines, T. R. *et al.* Local Innate Immune Responses and Influenza Virus Transmission and Virulence in Ferrets. *Journal of Infectious Diseases* **205**, 474–485 (2011).

42. Schmittgen, T. D. & Zakrajsek, B. A. Effect of experimental treatment on housekeeping gene expression: validation by real-time, quantitative RT-PCR. *J. Biochem. Biophys. Methods* **46**, 69–81 (2000).

43. Marcelin, G. *et al.* Fatal Outcome of Pandemic H1N1 2009 Influenza Virus Infection Is Associated with Immunopathology and Impaired Lung Repair, Not Enhanced Viral Burden, in Pregnant Mice. *Journal of Virology* **85**, 11208–11219 (2011).

44. Yu, X. *et al.* Intensive Cytokine induction in Pandemic H1N1 Influenza Virus Infection Accompanied by Robust Production of IL-10 and IL-6. *PLoS ONE* **6**, e28680 (2011).

45. Lai, C. F. *et al.* Receptors for interleukin (IL)-10 and IL-6-type cytokines use similar signaling mechanisms for inducing transcription through IL-6 response elements. *J. Biol. Chem.* **271**, 13968–13975 (1996).

46. Terai, M. *et al.* Interleukin 6 mediates production of interleukin 10 in metastatic melanoma. *Cancer Immunol. Immunother.* **61**, 145–155 (2012).

47. Gabay, C. & Kushner, I. Acute-phase proteins and other systemic responses to inflammation. *N. Engl. J. Med.* **340**, 448–454 (1999).

48. Lin, W.-C., Lin, C.-F., Chen, C.-L., Chen, C.-W. & Lin, Y.-S. Prediction of outcome in patients with acute respiratory distress syndrome by bronchoalveolar lavage inflammatory mediators. *Experimental Biology and Medicine* **235**, 57–65 (2010).

49. Wang, S. *et al.* Influenza Virus–Cytokine‑Protease Cycle in the Pathogenesis of Vascular Hyperpermeability in Severe Influenza. *The Journal of Infectious Diseases* **202**, 991–1001 (2010).

50. Ding, H. *et al.* Influenza vaccination coverage among pregnant women–National 2009 H1N1 Flu Survey (NHFS). *American Journal of Obstetrics and Gynecology* **204**, S96–S106 (2011).